

# **Topological insulator thin film properties**

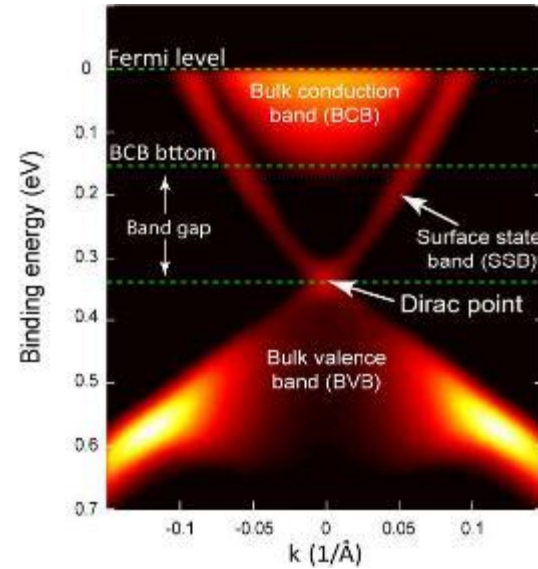
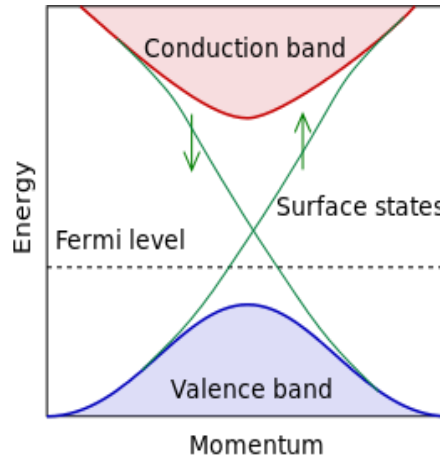
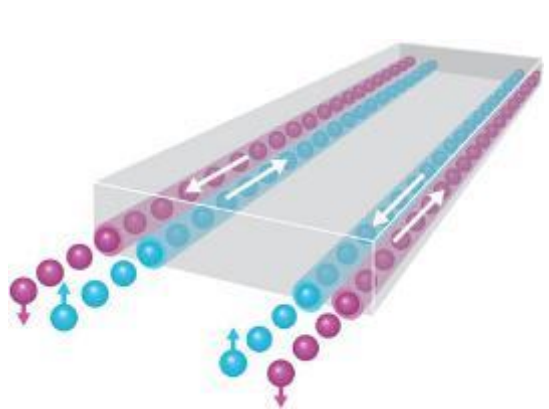
Ko-Hsuan Chen  
Chun-Chia Chen

2019.11.14

# Outline

- Introduction to 3D topological insulator
- Common ways to make thin films and introduction to epitaxy
- Paper review: properties found in TI thin films
- Van der Waals epitaxy of topological insulator  $\text{Bi}_2\text{Se}_3$  on single layer transition metal dichalcogenide  $\text{MoS}_2$
- Crystal growth and electronic band structure of  $\alpha$ -Sn thin films
- Thin film growth of topological insulators  $\text{Bi}_2\text{Se}_3$  and  $(\text{Bi},\text{Sb})_2\text{Te}_3$  toward bulk-insulating features and enhanced interfacial exchange coupling on rare earth iron garnets

# Introduction of topological insulators (TIs)



Electronic band structure along the K- $\Gamma$ -K direction of undoped  $\text{Bi}_2\text{Se}_3$  by ARPES, Y. L. Chen et al, Science, (2010).

## Properties

- Strong spin-orbital coupling
- Spin momentum locked surface state protected by time reversal symmetry

## Applications

- Spin momentum locked surface state - spintronics device
- Interface of TI and superconductor - Majorana fermion, quantum computation

# Tools for studying the properties of topological insulators

## Material properties

- Crystal structure
  - X-ray diffraction
  - RHEED, LEED
  - TEM
  - ...
- Chemical composition
  - XPS
  - EDX
  - ...
- Surface morphology
  - AFM
  - STM

## Physical properties

- Electrical transport properties
  - Hall measurement
    - High mobility
    - Weak antilocalization (spin-momentum locking)
- Electronic band structure
  - ARPES
    - Direct image of topological surface state in reciprocal space
  - STS

Topological  
insulators

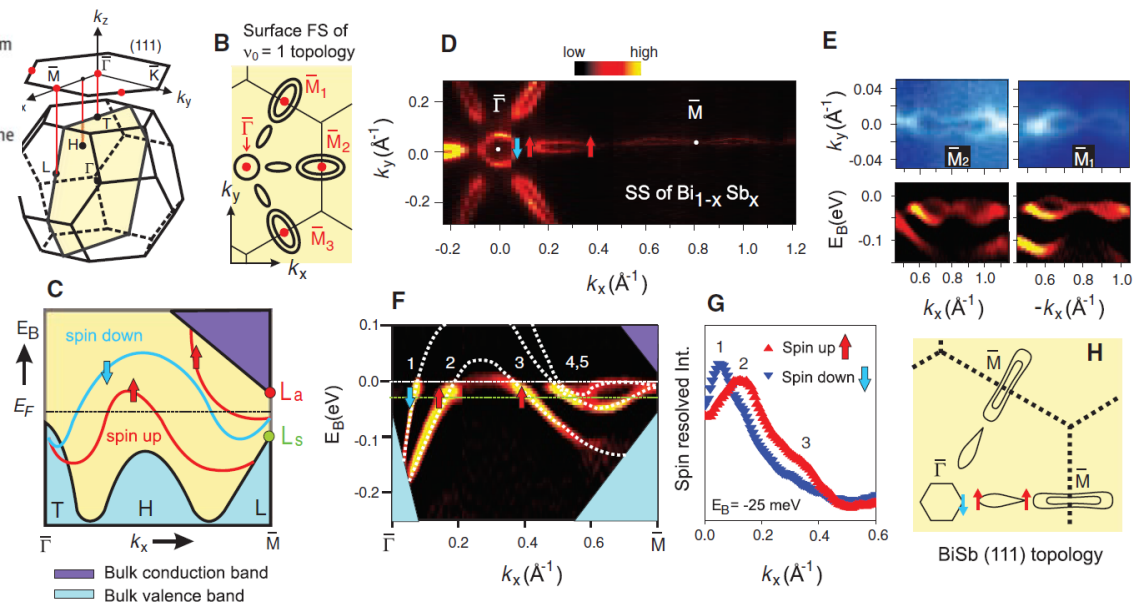
# First 3D TI (first generation)

## Observation of Unconventional Quantum Spin Textures in Topological Insulators

D. Hsieh,<sup>1</sup> Y. Xia,<sup>1,2</sup> L. Wray,<sup>1,3</sup> D. Qian,<sup>1</sup> A. Pal,<sup>1</sup> J. H. Dil,<sup>4,5</sup> J. Osterwalder,<sup>5</sup> F. Meier,<sup>4,5</sup> G. Bihlmayer,<sup>6</sup> C. L. Kane,<sup>7</sup> Y. S. Hor,<sup>8</sup> R. J. Cava,<sup>8</sup> M. Z. Hasan<sup>1,2\*</sup>

A topologically ordered material is characterized by a rare quantum organization of electrons that evades the conventional spontaneously broken symmetry-based classification of condensed matter. Exotic spin-transport phenomena, such as the dissipationless quantum spin Hall effect, have been speculated to originate from a topological order whose identification requires a spin-sensitive measurement, which does not exist to this date in any system. Using Mott polarimetry, we probed the spin degrees of freedom and demonstrated that topological quantum numbers are completely determined from spin texture-imaging measurements. Applying this method to Sb and  $\text{Bi}_{1-x}\text{Sb}_x$ , we identified the origin of its topological order and unusual chiral properties. These results taken together constitute the first observation of surface electrons collectively carrying a topological quantum Berry's phase and definite spin chirality, which are the key electronic properties component for realizing topological quantum computing bits with intrinsic spin Hall-like topological phenomena.

Single crystal



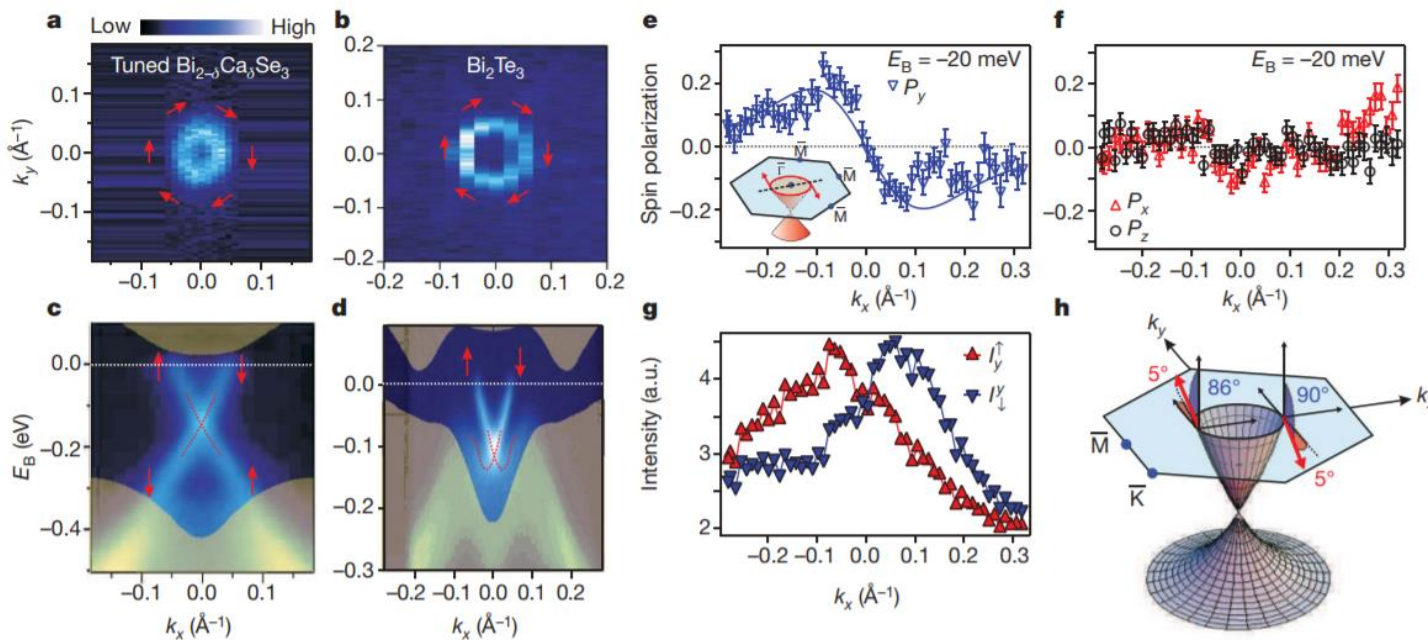
D. Hsieh et al., Science 323, 919 (2009).

# $\text{Bi}_2\text{Se}_3$ family 3D TI (second generation)

## A tunable topological insulator in the spin helical Dirac transport regime

Single crystal

D. Hsieh<sup>1</sup>, Y. Xia<sup>1</sup>, D. Qian<sup>1,5</sup>, L. Wray<sup>1</sup>, J. H. Dil<sup>6,7</sup>, F. Meier<sup>6,7</sup>, J. Osterwalder<sup>7</sup>, L. Patthey<sup>6</sup>, J. G. Checkelsky<sup>1</sup>, N. P. Ong<sup>1</sup>, A. V. Fedorov<sup>8</sup>, H. Lin<sup>9</sup>, A. Bansil<sup>9</sup>, D. Grauer<sup>2</sup>, Y. S. Hor<sup>2</sup>, R. J. Cava<sup>2</sup> & M. Z. Hasan<sup>1,3,4</sup>



# Topological insulators material

- **Bi<sub>2</sub>Se<sub>3</sub> family** and related materials: Both conduction and valence band consist of *p* orbitals
  - Bi<sub>2</sub>Se<sub>3</sub> family
  - TIBiSe<sub>2</sub>
  - LaBiTe<sub>3</sub>
  - PbBi<sub>2</sub>Se<sub>4</sub>
- **HgTe** and related materials: S-type  $\Gamma_6$  band and p-type  $\Gamma_8$  band
  - HgTe quantum wells and strained bulk HgTe, HgSe,  $\beta$ -HgS
  - AlSb/InAs/GaSb quantum wells
  - Heusler compounds
  - Chalcopyrite semiconductors
  - $\alpha$ - and  $\beta$ -Ag<sub>2</sub>Te
  - Skutterudites and filled skutterudites
- Other materials
  - Bi<sub>x</sub>Sb<sub>1-x</sub>
  - Graphene, silicene, and related material
  - PbTe, SnTe, and related material
  - Correlated materials with d or f orbitals

Periodic Table of the Elements

1	H	Hydrogen	1.01
2	He	Helium	4.00
3	Li	Lithium	6.94
4	Be	Boron	9.01
5	Na	Sodium	22.99
6	Mg	Magnesium	24.31
7	K	Potassium	39.10
8	Ca	Calcium	40.08
9	Sc	Scandium	44.96
10	Ti	Titanium	47.88
11	V	Vanadium	50.94
12	Cr	Chromium	51.99
13	Mn	Manganese	54.94
14	Fe	Iron	55.85
15	Co	Cobalt	58.93
16	Ni	Nickel	58.69
17	Cu	Copper	63.55
18	Zn	Zinc	65.38
19	Al	Aluminum	26.98
20	Si	Silicon	28.09
21	P	Phosphorus	30.97
22	S	Sulfur	32.06
23	Cl	Chlorine	35.45
24	Ar	Argon	39.95
25	B	Boron	10.81
26	C	Carbon	12.01
27	N	Nitrogen	14.01
28	O	Oxygen	16.00
29	F	Fluorine	19.00
30	Ne	Neon	20.18
31	Ga	Gallium	69.72
32	Ge	Germanium	72.63
33	As	Arsenic	74.92
34	Se	Selenium	78.97
35	Br	Bromine	79.90
36	Kr	Krypton	83.80
37	Rb	Rubidium	85.47
38	Sr	Samarium	87.62
39	Y	Yttrium	88.91
40	Zr	Zirconium	91.22
41	Nb	Niobium	92.91
42	Mo	Molybdenum	95.95
43	Tc	Technetium	98.91
44	Ru	Ruthenium	101.07
45	Rh	Rhodium	102.91
46	Pd	Palladium	106.42
47	Ag	Silver	107.87
48	Cd	Cadmium	114.41
49	In	Indium	114.82
50	Sn	Tin	118.71
51	Sb	Antimony	121.76
52	Te	Tellurium	127.6
53	I	Iodine	126.90
54	Xe	Xenon	131.29
55	Cs	Cesium	132.91
56	Ba	Boron	137.33
57	Hf	Hafnium	178.49
58	Ta	Tantalum	180.95
59	W	Tungsten	183.85
60	Re	Rhenium	186.21
61	Os	Osmium	190.23
62	Ir	IrIDIUM	192.22
63	Pt	Platinum	195.08
64	Au	Gold	196.97
65	Hg	Mercury	200.59
66	Tl	Thallium	204.38
67	Pb	Lead	207.20
68	Bi	Bismuth	209.98
69	Po	Poison	222.02
70	At	Actinium	220.98
71	Rn	Rutherfordium	222.02
72	Ts	Technetium	224.03
73	Fr	Francium	223.02
74	Ra	Radium	226.03
75	Rf	Rutherfordium	261.01
76	Dy	Dysprosium	262.01
77	Db	Dubnium	262.01
78	Sg	Singapore	262.01
79	Bh	Berillium	264.01
80	Hs	Hassium	269.01
81	Mt	Moscovium	278.01
82	Ds	Darmstadtium	281.01
83	Rg	Rutherfordium	285.01
84	Cn	Coincidence	286.01
85	Nh	Nihonium	286.01
86	Fl	Flerovium	289.01
87	Mc	Moscovium	289.01
88	Lv	Livermorium	293.01
89	Ts	Technetium	294.01
90	Fr	Francesium	294.01
91	Th	Thorium	232.04
92	Pa	Protactinium	231.04
93	U	Uranium	238.03
94	Np	Neptunium	237.05
95	Pm	Plutonium	240.06
96	Am	Americium	243.06
97	Cm	Cerium	247.07
98	Bk	Berkelium	251.08
99	Es	Einsteinium	254.01
100	Fm	Fermium	258.10
101	Md	Mendelevium	259.10
102	No	Nobelium	262.01
103	Lr	Lanthanum	262.01
104	Ts	Technetium	294.01
105	Fr	Francesium	294.01
106	Db	Dubnium	262.01
107	Sg	Singapore	262.01
108	Bh	Berillium	264.01
109	Hs	Hassium	269.01
110	Mt	Moscovium	278.01
111	Rg	Rutherfordium	285.01
112	Cn	Coincidence	286.01
113	Nh	Nihonium	286.01
114	Fl	Flerovium	289.01
115	Mc	Moscovium	289.01
116	Lv	Livermorium	293.01
117	Ts	Technetium	294.01
118	Og	Oganesson	294.01

# Bulk crystals versus thin films

## Bulk crystals

### Advantages:

- Usually easier to achieve
- Higher crystal quality and less defects
- Usually easier to prepare the fresh surface by cleaving for measurements such as ARPES, STM etc.

→ Faster in characterizing the topological phases/states of materials

### Disadvantages:

- Hard to integrate with other materials for possible application for advance technologies
- Usually harder to study the properties in ultra thin regime

## Thin film

### Advantages:

- Usually easier to combine with other materials for the study of novel physical properties at the interface such as magnetic proximity effect in TI/magnetic material, majorana bound states in TI/SC etc.
- Easy to study the properties through a wide range of thickness, for example transport properties with electrical field effect
- Have chances to integrate with current Si technology or other industrial applications

### Disadvantages:

- More complicated material issue need to be considered during growth, such as substrate selection, growth methods

# Outline

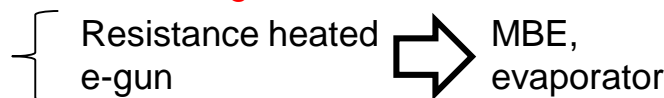
- Introduction to 3D topological insulator
- Common ways to make thin films and introduction to epitaxy
- Paper review: properties found in TI thin films
- Van der Waals epitaxy of topological insulator  $\text{Bi}_2\text{Se}_3$  on single layer transition metal dichalcogenide  $\text{MoS}_2$
- Crystal growth and electronic band structure of  $\alpha\text{-Sn}$  thin films
- Thin film growth of topological insulators  $\text{Bi}_2\text{Se}_3$  and  $(\text{Bi},\text{Sb})_2\text{Te}_3$  toward bulk-insulating features and enhanced interfacial exchange coupling on rare earth iron garnets

# Common ways of making thin films

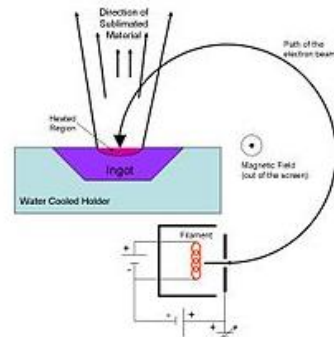
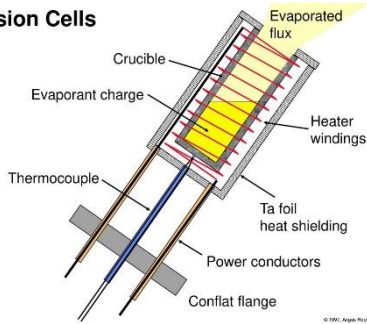
## Physical Vapor Deposition (PVD)

### Evaporation

Source material (bulk) → atoms  
Heating



### Effusion Cells



### Sputtering

Target (Bulk) → atoms

Gas ion collision

Glowing/Plasma

## Chemical Vapor Deposition (CVD)

one or more volatile **precursors**, which **react** and/or decompose on the substrate surface to produce the desired thin films

### example

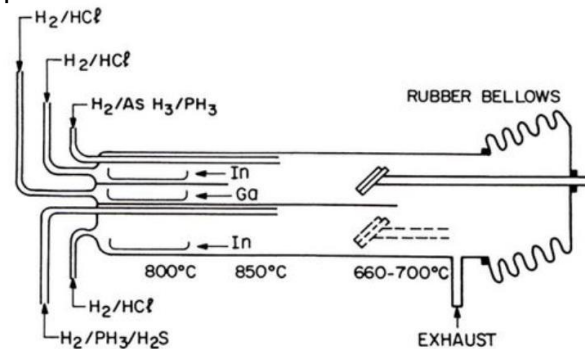
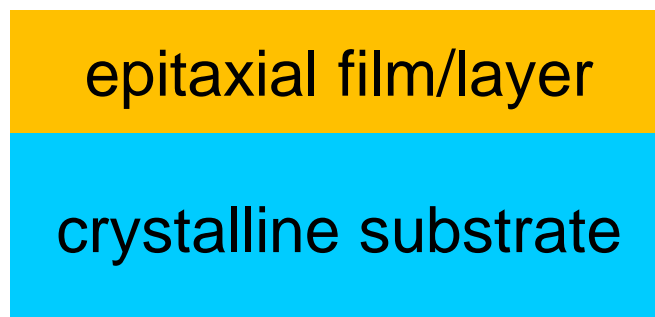


Figure 4-3. Schematic of atmospheric CVD reactor used to grow GaAs and other compound semiconductor films by the hydride process. (Reprinted with permission from Ref. 10).

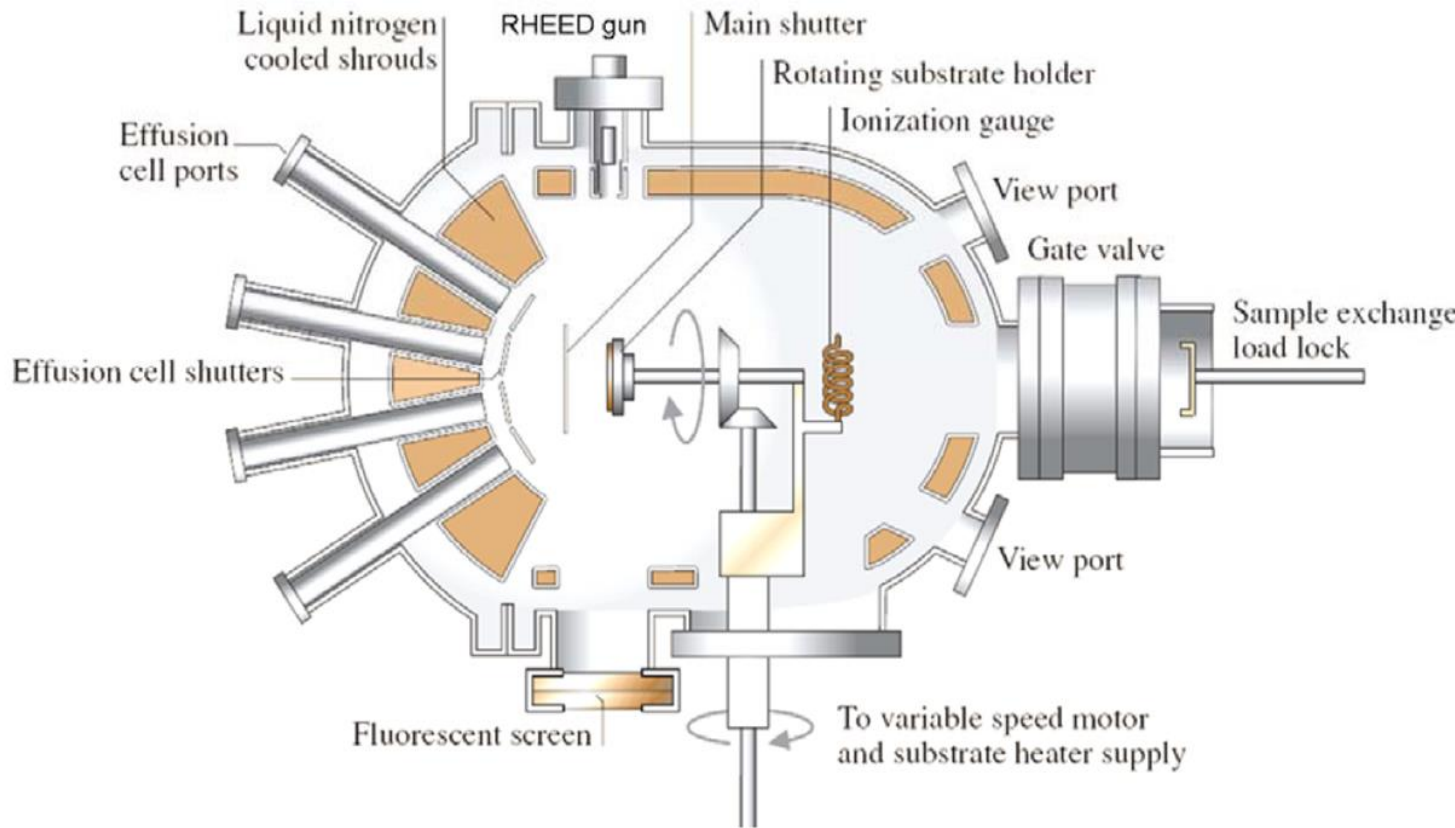
APCVD  
LPCVD  
MOCVD  
ALD  
....

# Introduction to epitaxy

- The term epitaxy comes from the Greek roots **epi**, meaning "above", and **taxis**, meaning "in ordered manner".
- **Homoepitaxy**
  - Substrate and film are the same material.
- **Heteroepitaxy**
  - Substrate and film are different materials.



# Molecular Beam Epitaxy



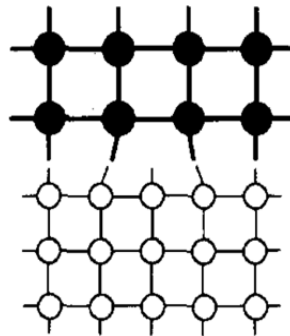
## Advantages:

- Clean (UHV)
- Low and well- controlled growth rate
- Precise thickness control down to ML

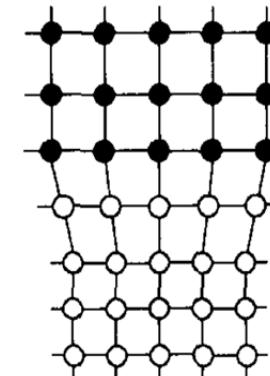
# Heteroepitaxy

## Covalent epitaxy

3D material



3D material

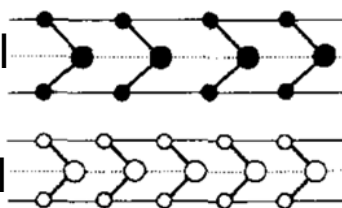


dangling bonds

intermediate layer

## Van der Waals epitaxy

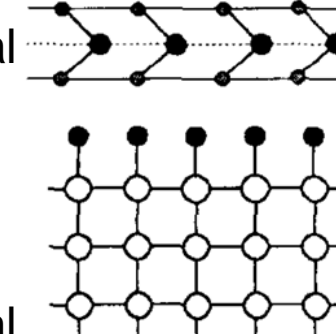
2D material



van der Waals gap

2D material

2D material



quasi van der Waals gap

3D material

The lattice matching issue in epitaxy can be naturally overcome because of the layered structure of 2D materials.

A. Koma, Thin Solid Films 216, 72 (1992).

# Outline

- Introduction to 3D topological insulator
- Common ways to make thin films and introduction to epitaxy
- Paper review: properties found in TI thin films
- Van der Waals epitaxy of topological insulator  $\text{Bi}_2\text{Se}_3$  on single layer transition metal dichalcogenide  $\text{MoS}_2$
- Crystal growth and electronic band structure of  $\alpha\text{-Sn}$  thin films
- Thin film growth of topological insulators  $\text{Bi}_2\text{Se}_3$  and  $(\text{Bi},\text{Sb})_2\text{Te}_3$  toward bulk-insulating features and enhanced interfacial exchange coupling on rare earth iron garnets

# Thickness limit of 3D-TIs

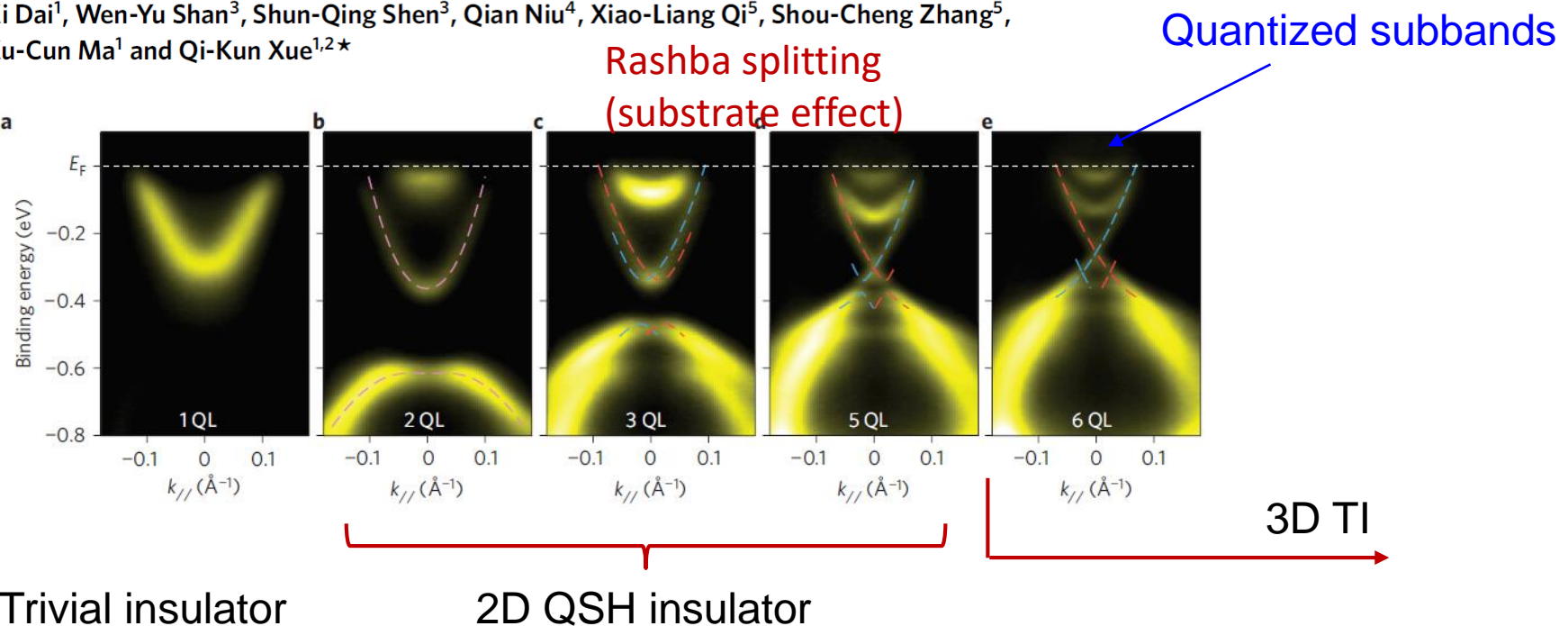
LETTERS

nature  
physics

PUBLISHED ONLINE: 13 JUNE 2010 | DOI:10.1038/NPHYS1689

## Crossover of the three-dimensional topological insulator $\text{Bi}_2\text{Se}_3$ to the two-dimensional limit

Yi Zhang<sup>1</sup>, Ke He<sup>1\*</sup>, Cui-Zu Chang<sup>1,2</sup>, Can-Li Song<sup>1,2</sup>, Li-Li Wang<sup>1</sup>, Xi Chen<sup>2</sup>, Jin-Feng Jia<sup>2</sup>, Zhong Fang<sup>1</sup>,  
Xi Dai<sup>1</sup>, Wen-Yu Shan<sup>3</sup>, Shun-Qing Shen<sup>3</sup>, Qian Niu<sup>4</sup>, Xiao-Liang Qi<sup>5</sup>, Shou-Cheng Zhang<sup>5</sup>,  
Xu-Cun Ma<sup>1</sup> and Qi-Kun Xue<sup>1,2\*</sup>



$$E_{\sigma\pm}(k_{\parallel}) = E_0 - Dk_{\parallel}^2 \pm \sqrt{(|\tilde{V}'| + \sigma v_F \hbar k_{\parallel})^2 + \left(\frac{\Delta}{2} - Bk_{\parallel}^2\right)^2}$$

# Thickness limit of 3D-TIs

## Intrinsic Topological Insulator $\text{Bi}_2\text{Te}_3$ Thin Films on Si and Their Thickness Limit

By Yao-Yi Li, Guang Wang, Xie-Gang Zhu, Min-Hao Liu, Cun Ye, Xi Chen, Ya-Yu Wang, Ke He, Li-Li Wang, Xu-Cun Ma, Hai-Jun Zhang, Xi Dai, Zhong Fang, Xin-Cheng Xie, Ying Liu, Xiao-Liang Qi, Jin-Feng Jia,\* Shou-Cheng Zhang, and Qi-Kun Xue

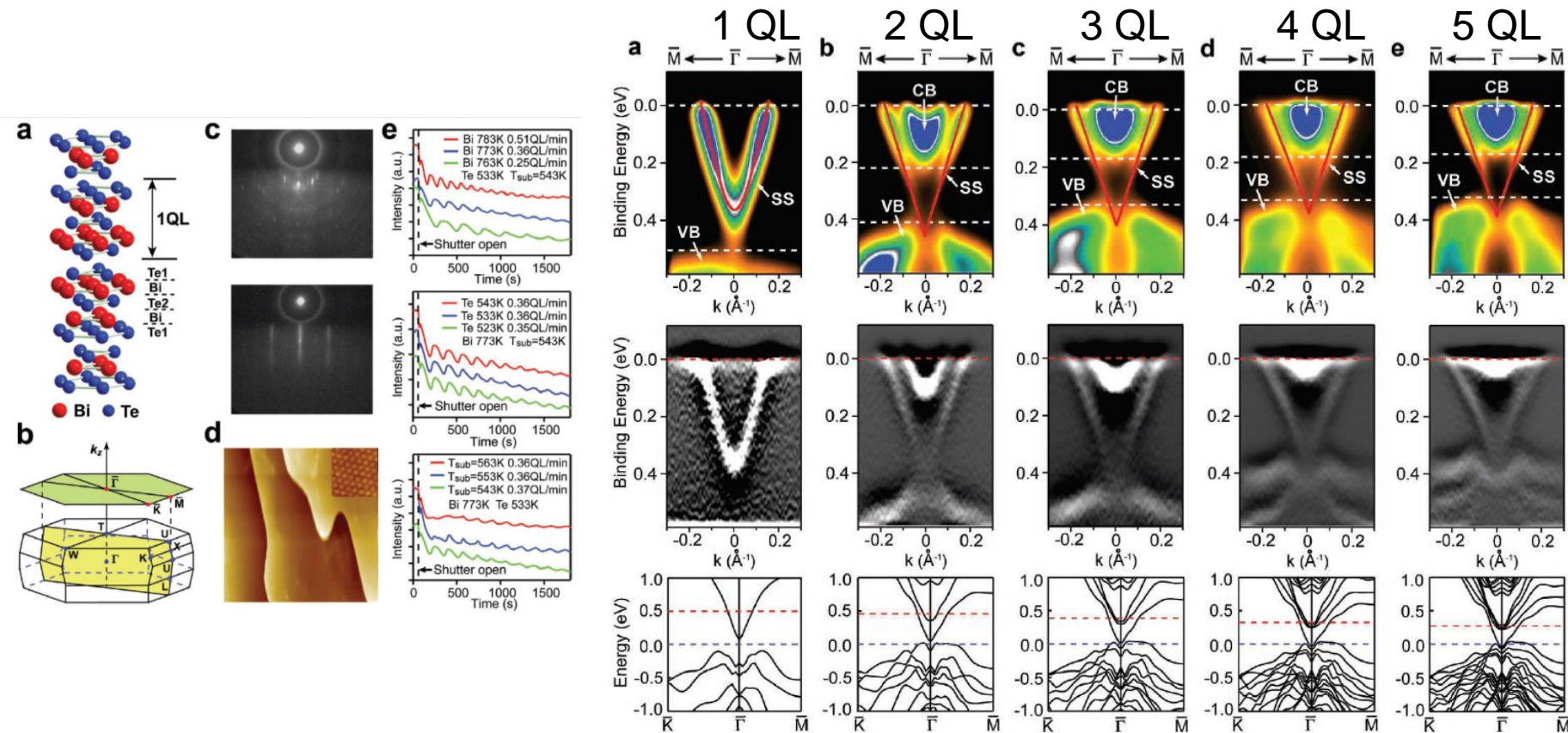


Figure 3. Band structure of ultrathin films of  $\text{Bi}_2\text{Te}_3$ . a) 1 QL. b) 2 QL. c) 3 QL. d) 4 QL. e) 5 QL. All the spectra were taken along the  $\overline{\Gamma}-\overline{M}$  direction. Upper panels: ARPE intensity maps; Middle panels: differential ARPE intensity maps; Lower panels: band structures from first-principles calculations. If the Fermi level (blue dashed line) in the calculated band structure (lower panels) is shifted to higher energy (red dashed line), the major features seen in the middle panels are well reproduced.

# Observation of quantum Hall effect in $\text{Bi}_2\text{Se}_3$ thin film

NANO  
LETTERS

Letter

pubs.acs.org/NanoLett

## Record Surface State Mobility and Quantum Hall Effect in Topological Insulator Thin Films via Interface Engineering

Nikesh Koirala,<sup>†</sup> Matthew Brahlek,<sup>†</sup> Maryam Salehi,<sup>‡</sup> Liang Wu,<sup>§</sup> Jixia Dai,<sup>†</sup> Justin Waugh,<sup>||</sup> Thomas Nummy,<sup>||</sup> Myung-Geun Han,<sup>†</sup> Jisoo Moon,<sup>†</sup> Yimei Zhu,<sup>†</sup> Daniel Dessau,<sup>||</sup> Weida Wu,<sup>†</sup> N. Peter Armitage,<sup>§</sup> and Seongshik Oh<sup>\*†</sup>

<sup>†</sup>Department of Physics and Astronomy and <sup>‡</sup>Department of Materials Science and Engineering, Rutgers, The State University of New Jersey, Piscataway, New Jersey 08854, United States

<sup>§</sup>Department of Physics and Astronomy, The Johns Hopkins University, Baltimore, Maryland 21218, United States

<sup>||</sup>Department of Physics, University of Colorado, Boulder, Colorado 80309, United States

<sup>†</sup>Condensed Matter Physics and Materials Science, Brookhaven National Lab, Upton, New York 11973, United States

Supporting Information

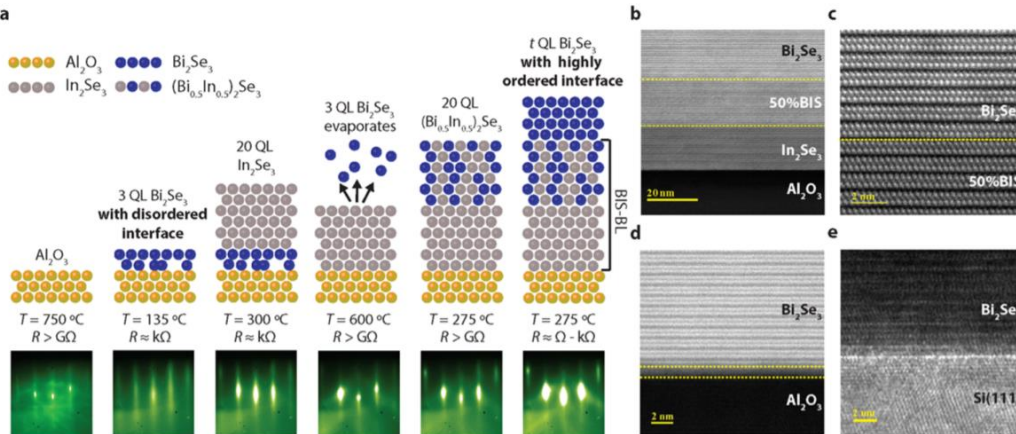


Figure 1. Growth process of  $\text{Bi}_2\text{Se}_3$  films on the 20 QL  $\text{In}_2\text{Se}_3$ /20 QL  $(\text{Bi}_{0.5}\text{In}_{0.5})_2\text{Se}_3$  buffer layer (BIS-BL) and comparison with films grown on  $\text{Al}_2\text{O}_3(0001)$  and  $\text{Si}(111)$ . (a) Cartoon showing each stage of film growth along with the corresponding growth temperature ( $T$ ), sheet resistance ( $R$ ) and RHEED images. HAADF-STEM image of  $\text{Bi}_2\text{Se}_3$  grown on (b) BIS-BL, which (c) shows an atomically sharp interface between  $\text{Bi}_2\text{Se}_3$  and BIS-BL, while (d)  $\text{Bi}_2\text{Se}_3$  grown directly on  $\text{Al}_2\text{O}_3(0001)$  has clearly disordered interface. (e) TEM image of  $\text{Bi}_2\text{Se}_3$  grown on  $\text{Si}(111)$  (from ref 13). In (b,c),  $(\text{Bi}_{0.5}\text{In}_{0.5})_2\text{Se}_3$  is written as 50%BIS.

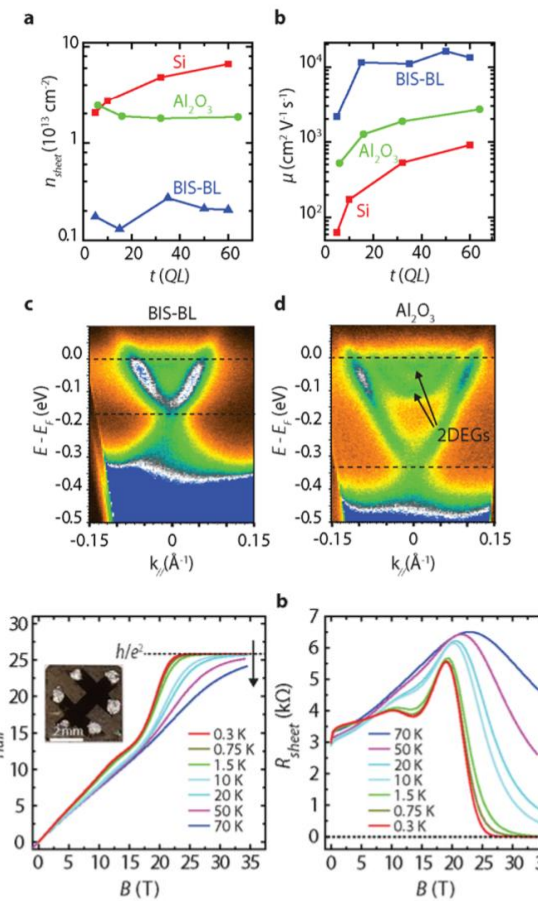


Figure 4. QHE in an 8 QL thick  $\text{Bi}_2\text{Se}_3$  film grown on BIS-BL and capped by both  $\text{MoO}_3$  and Se. (a) Hall resistance at different temperatures in magnetic field up to 34.5 T, which quantizes to  $(1.00000 \pm 0.00004)h/e^2$  ( $25813 \pm 1 \Omega$ ) at low temperatures. The inset shows the Hall-bar pattern of the measured film. (b) Corresponding longitudinal sheet resistance, which drops to zero ( $0 \pm 0.5 \Omega$ ) when Hall resistance quantizes to  $h/e^2$ . The vertical arrows indicate the direction of increasing temperature.

# Observation of quantum Hall effect in $(\text{Bi}_{0.53}\text{Sb}_{0.47})_2\text{Te}_3$ thin film

APPLIED PHYSICS LETTERS 110, 212401 (2017)



## Observation of Quantum Hall effect in an ultra-thin $(\text{Bi}_{0.53}\text{Sb}_{0.47})_2\text{Te}_3$ film

Wenqin Zou,<sup>1,a)</sup> Wei Wang,<sup>2,a)</sup> Xufeng Kou,<sup>3</sup> Murong Lang,<sup>3</sup> Yabin Fan,<sup>3</sup> Eun Sang Choi,<sup>4</sup> Alexei V. Fedorov,<sup>5</sup> Kejie Wang,<sup>2</sup> Liang He,<sup>2,3,b)</sup> Yongbing Xu,<sup>2,b)</sup> and Kang. L. Wang<sup>3,b)</sup>

<sup>1</sup>National Lab of Solid State Microstructures, Department of Physics, Nanjing University, Nanjing 210093, People's Republic of China

<sup>2</sup>York-Nanjing Joint Center (YNJC) for Spintronics and Nano Engineering, School of Electronics Science and Engineering, Nanjing University, Nanjing 210093, China

<sup>3</sup>Department of Electrical Engineering, University of California, Los Angeles, Los Angeles, California 90095, USA

<sup>4</sup>National High Magnetic Field Laboratory, Tallahassee, Florida 32310, USA

<sup>5</sup>Advanced Light Source Division, Lawrence Berkeley national laboratory, 1 Cyclotron Road, Berkeley, California 94720, USA

(Received 5 November 2016; accepted 2 April 2017; published online 22 May 2017)

We report the observation of the Quantum Hall effect from the topological surface states in both the Dirac electron and Dirac hole regions in a 4 quintuple layer  $(\text{Bi}_{0.53}\text{Sb}_{0.47})_2\text{Te}_3$  film grown on GaAs (111)B substrates. The Fermi level is sitting within the enlarged bulk band gap due to the quantum confinement of the ultra-thin film and can be tuned through the Dirac point by gate biases. Furthermore, the Hall resistance  $R_{xy}$  shows even denominator plateaus, which could be fractional Quantum Hall states. This may be due to the hybridization between the top and bottom surface states and suggests the possible way to manipulate the interaction of two surfaces for potential spintronic devices. Published by AIP Publishing. [http://dx.doi.org/10.1063/1.4983684]

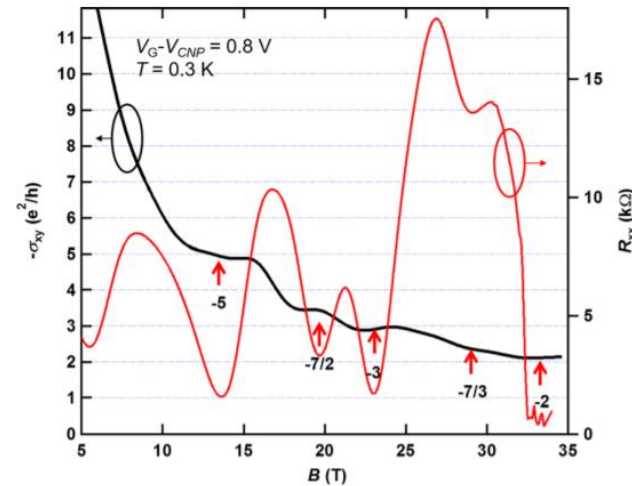
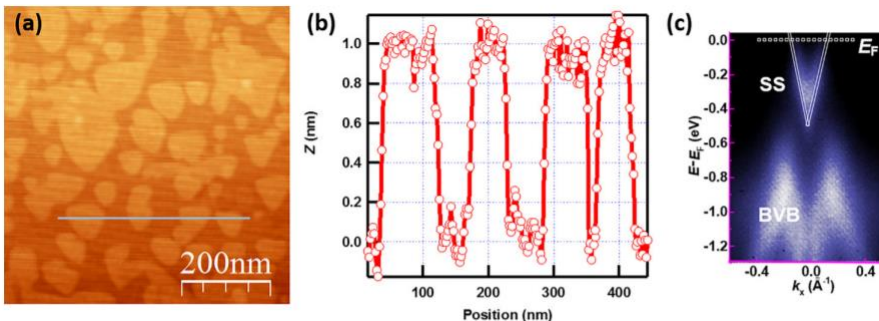


FIG. 3. Fractional quantum hall effect of  $(\text{Bi}_{0.53}\text{Sb}_{0.47})_2\text{Te}_3$  at a high field. (Left) The Hall conductivity  $\sigma_{xy}$  at  $V_G - V_{CNP} = 0.8$  V; the plateaus in  $\sigma_{xy}$  can be observed clearly. The Landau filling factors are also marked. (Right) The oscillations of the longitudinal resistance  $R_{xx}$ .

# p-n junction



ARTICLE

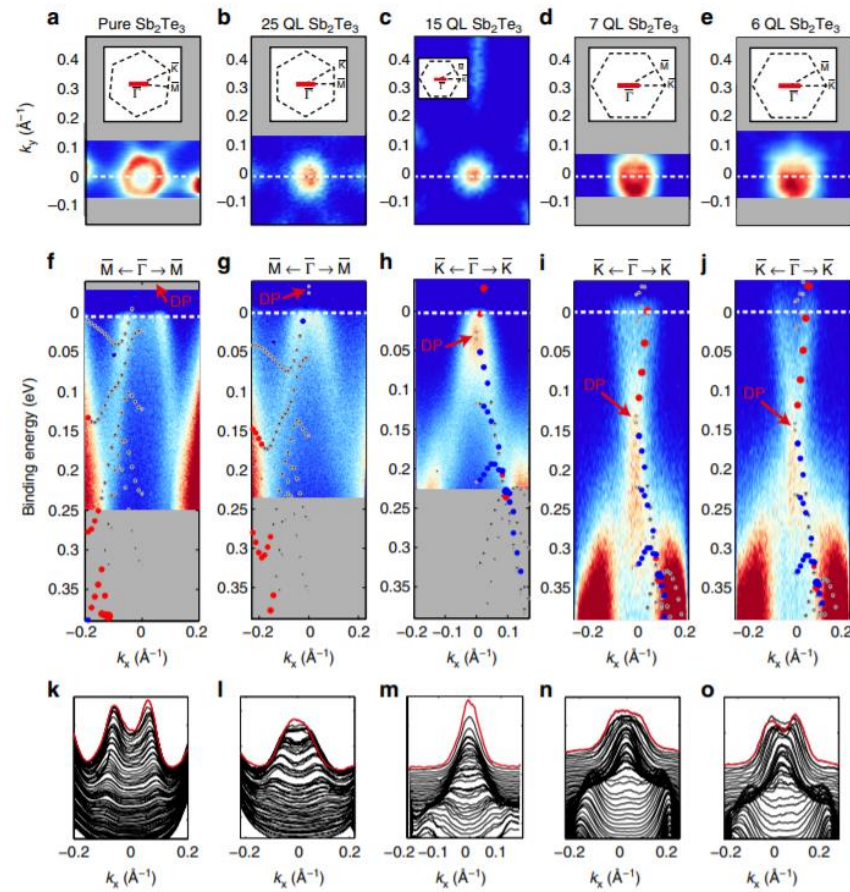
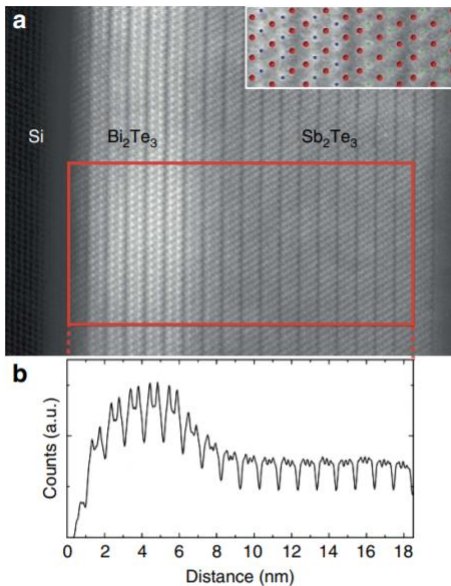
Received 8 May 2015 | Accepted 6 Oct 2015 | Published 17 Nov 2015

DOI: 10.1038/ncomms9816

OPEN

## Realization of a vertical topological p-n junction in epitaxial Sb<sub>2</sub>Te<sub>3</sub>/Bi<sub>2</sub>Te<sub>3</sub> heterostructures

Markus Eschbach<sup>1</sup>, Ewa Młyńczak<sup>1,2</sup>, Jens Kellner<sup>3</sup>, Jörn Kampmeier<sup>4</sup>, Martin Lanius<sup>4</sup>, Elmar Neumann<sup>5</sup>, Christian Weyrich<sup>4</sup>, Mathias Gehlmann<sup>1</sup>, Pika Gospodarić<sup>1</sup>, Sven Döring<sup>1</sup>, Gregor Mussler<sup>4</sup>, Nataliya Demarina<sup>6</sup>, Martina Luysberg<sup>5,7</sup>, Gustav Bihlmayer<sup>8</sup>, Thomas Schäpers<sup>4</sup>, Lukasz Plucinski<sup>1</sup>, Stefan Blügel<sup>8</sup>, Markus Morgenstern<sup>3</sup>, Claus M. Schneider<sup>1</sup> & Detlev Grützmacher<sup>4</sup>



# Magnetizing topological insulator via proximity effect

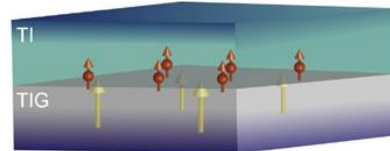
SCIENCE ADVANCES | RESEARCH ARTICLE

MATERIALS SCIENCE

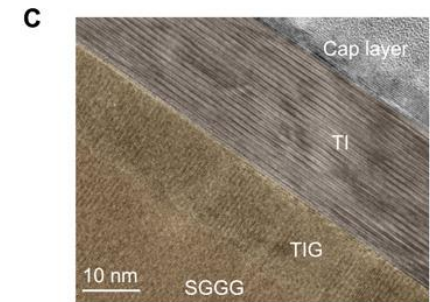
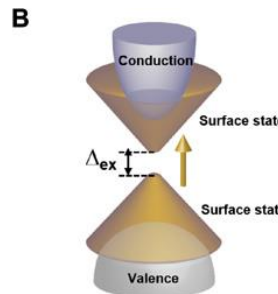
## Above 400-K robust perpendicular ferromagnetic phase in a topological insulator

Chi Tang,<sup>1\*</sup> Cui-Zu Chang,<sup>2,3\*</sup> Gejian Zhao,<sup>4</sup> Yawen Liu,<sup>1</sup> Zilong Jiang,<sup>1</sup> Chao-Xing Liu,<sup>3</sup> Martha R. McCartney,<sup>4</sup> David J. Smith,<sup>4</sup> Tingyong Chen,<sup>4</sup> Jagadeesh S. Moodera,<sup>2,5</sup> Jing Shi<sup>1†</sup>

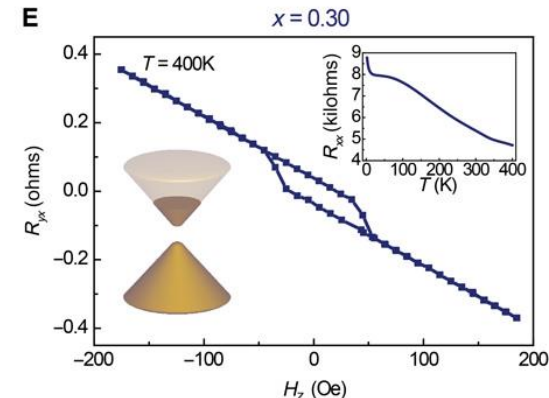
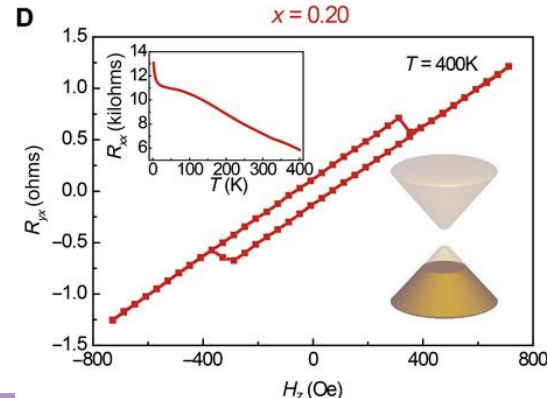
The quantum anomalous Hall effect (QAHE) that emerges under broken time-reversal symmetry in topological insulators (TIs) exhibits many fascinating physical properties for potential applications in nanoelectronics and spintronics. However, in transition metal-doped TIs, the only experimentally demonstrated QAHE system to date, the QAHE is lost at practically relevant temperatures. This constraint is imposed by the relatively low Curie temperature ( $T_c$ ) and inherent spin disorder associated with the random magnetic dopants. We demonstrate drastically enhanced  $T_c$  by exchange coupling TIs to  $\text{Tm}_3\text{Fe}_5\text{O}_{12}$ , a high- $T_c$  magnetic insulator with perpendicular magnetic anisotropy. Signatures showing that the TI surface states acquire robust ferromagnetism are revealed by distinct squared anomalous Hall hysteresis loops at 400 K. Point-contact Andreev reflection spectroscopy confirms that the TI surface is spin-polarized. The greatly enhanced  $T_c$ , absence of spin disorder, and perpendicular anisotropy are all essential to the occurrence of the QAHE at high temperatures.



Breaking time  
reversal symmetry  
in TI



Anomalous Hall effect in TI



# **Van der Waals epitaxy of topological insulator $\text{Bi}_2\text{Se}_3$ on single layer transition metal dichalcogenide $\text{MoS}_2$**

K. H. M. Chen *et al.*, *Appl. Phys. Lett.* **111**, 083106 (2017).



**Ko-Hsuan Mandy Chen, H. Y. Lin, S. R. Yang, C. Y. Wang, and J. Kwo**  
Dept. of Phys., National Tsing Hua Univ., Hsinchu, Taiwan

**X. Q. Zhang, and Y. H. Lee**  
Dept. of Mat. Sci. and Eng., National Tsing Hua Univ., Hsinchu, Taiwan

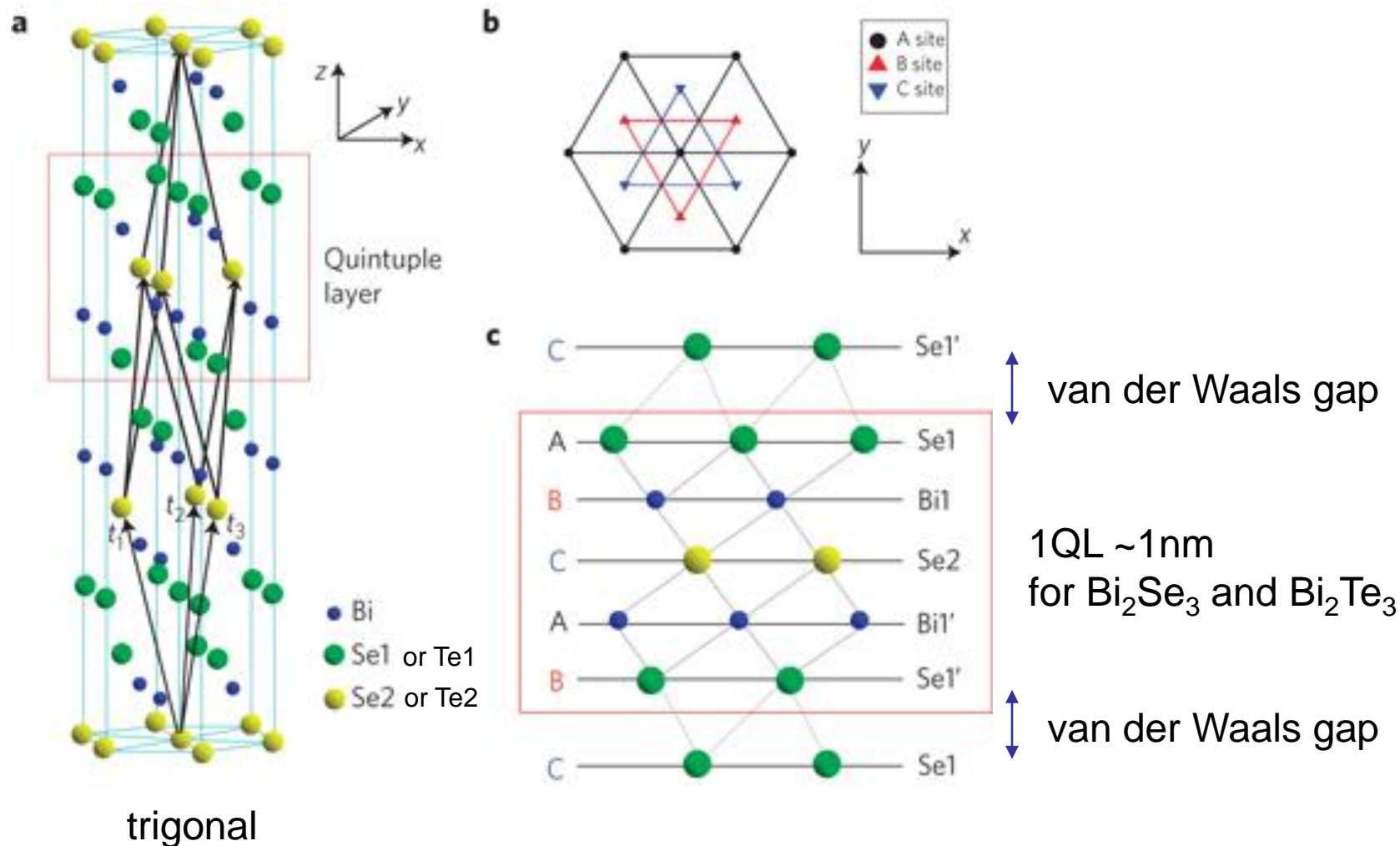


**C. K. Cheng, and M. Hong**  
Grad. Inst. of Appl. Phys., National Taiwan Univ., Taipei, Taiwan



**C. M. Cheng, and C. H. Hsu**  
National Synchrotron Radiation Research Center, Hsinchu, Taiwan

# Crystal structure of $\text{Bi}_2\text{Se}_3$ and $\text{Bi}_2\text{Te}_3$



H. Zhang et. al., Nat. Phys. 5 (6), 438 (2009)

# Motivation

## ■ Challenge in thin film

- High defect density such as Se vacancies
- Fermi level locates at conduction band easily

## ■ Other's work in $\text{Bi}_2\text{Se}_3$ thin film on different substrates

(refer to Prof. M. H. Xie's work in Chin. Phys. B, 22, 6, 068101 (2013))

- **non van der Waals type**

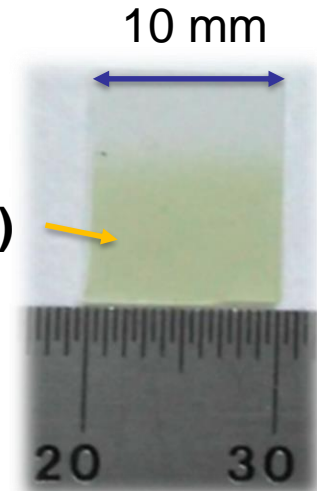
## How about inserting TMD material such as $\text{MoS}_2$ ?

- ✓ 2D layered structure
- ✓ hexagonal symmetry
- ✓ van der Waals type surface
- ✓ can be grown on diverse substrates
- **van der Waals type**  
graphene

# Sample Growth

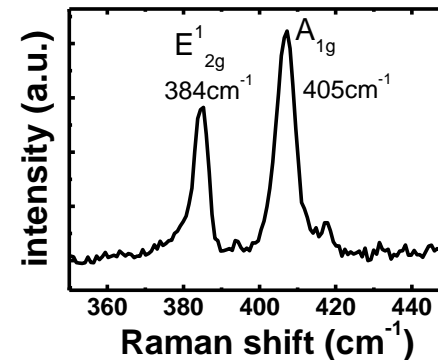
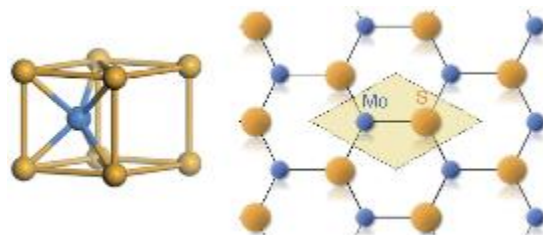
- clean  $\text{Al}_2\text{O}_3(0001)$  substrate  
surface roughness: 0.16nm

1.  $\text{H}_2\text{SO}_4:\text{H}_2\text{O}_2=1:1$  30 min
2. acetone 5min in ultrasonic bath
3. alcohol 5min in ultrasonic bath

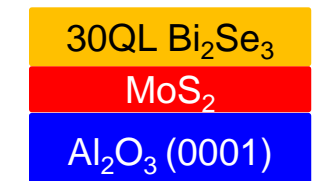


- grow  $\text{MoS}_2$  monolayer by chemical vapor deposition (CVD)

crystal structure: hexagonal P63/mmc  
lattice constant:  $a = 0.31 \text{ nm}$ ,  $c = 1.28 \text{ nm}$   
surface roughness: 0.15 nm  
typical triangular domain size:  $20\text{-}30 \mu\text{m}$   
large and continuous area up to 10 mm x 8 mm  
provided by Prof. Y. H. Lee's group in NTHU



Nature Comm., 10, 1038 (2012)  
Nano Lett., 12 (3), 1538-1544 (2012)



- grow  $\text{Bi}_2\text{Se}_3$  film by molecular beam epitaxy (MBE)  
rate:  $\sim 1 \text{ QL/min}$ , Se/Bi flux ratio: 20

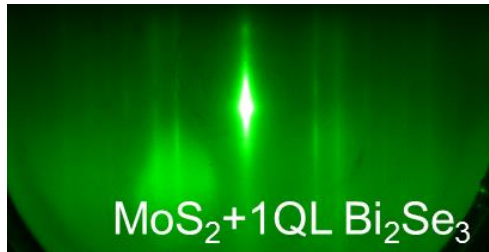
lattice mismatch: 15.7% ( $\text{Al}_2\text{O}_3$ ), -24.9% ( $\text{MoS}_2$ )

two step growth  
 $T_s = 180^\circ\text{C}/280^\circ\text{C}$

one step growth  
 $T_s = 280^\circ\text{C}$

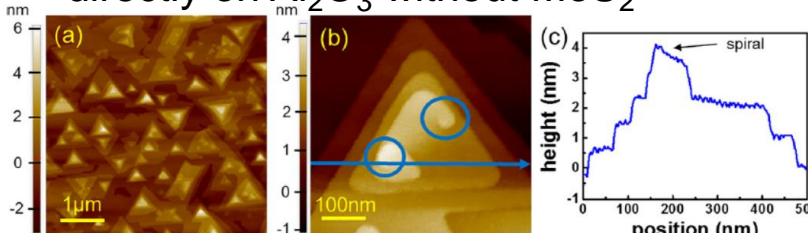
# High quality $\text{Bi}_2\text{Se}_3$ thin films using a $\text{MoS}_2$ template

Excellent crystallinity

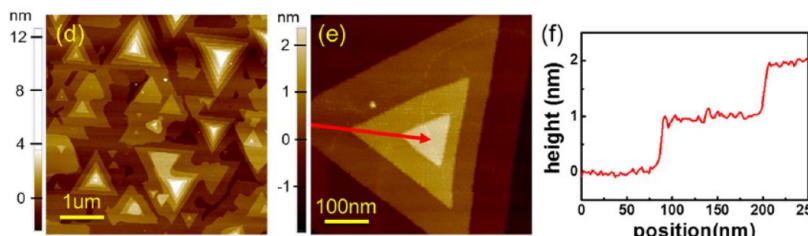


Large triangular shaped domain

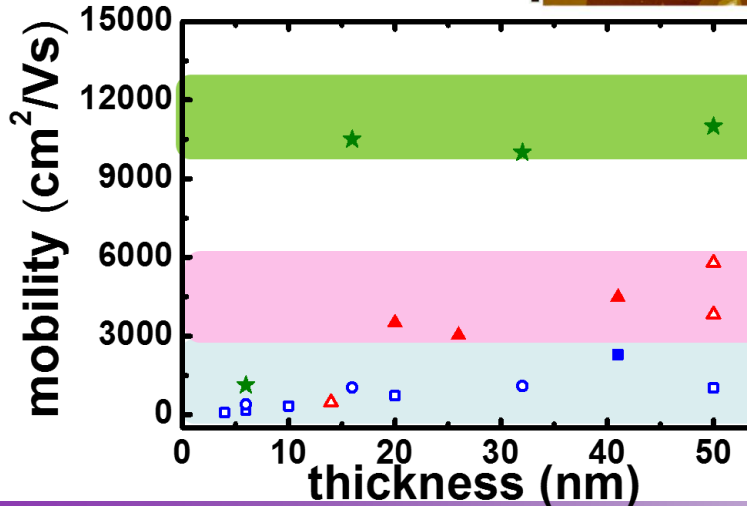
directly on  $\text{Al}_2\text{O}_3$  without  $\text{MoS}_2$



with  $\text{MoS}_2$  template

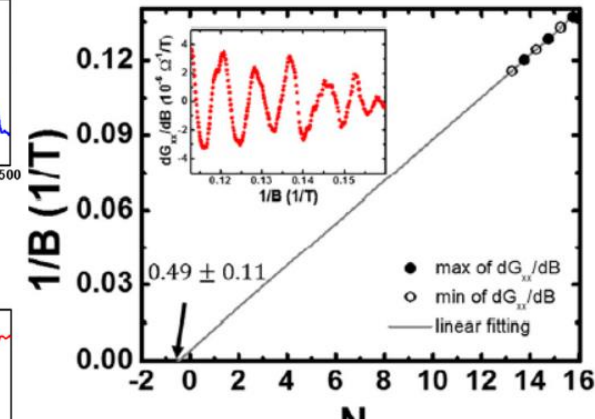


High mobility



- van der Waals type surface
  - good interface
  - good in-plane domain order
- van der Waals type surface
  - good interface
  - poor in-plane domain order
- non van der Waals type surface
  - poor interface
  - good in-plane order

SdH oscillation from topological surface state



○ on  $\text{Al}_2\text{O}_3$  (no capping)

★ on  $(\text{Bi}_x\text{In}_{1-x})_2\text{Se}_3/\text{Al}_2\text{O}_3$  (no capping)  
S. Oh et al, Nano Lett., 15 (12), 8245 (2015).

△ on  $\text{MoS}_2/\text{Al}_2\text{O}_3$  (no capping) our data

▲ on  $\text{MoS}_2/\text{Al}_2\text{O}_3$  (30 nm Se capping) our data

□ on  $\text{Al}_2\text{O}_3$  (no capping) our data

■ on  $\text{Al}_2\text{O}_3$  (30 nm Se capping) our data

# Crystal growth and electronic band structure of $\alpha$ -Sn thin films

**Ko-Hsuan (Mandy) Chen, H. Y. Lin, S. W. Huang, and J. Kwo\***

Dept. of Phys., National Tsing Hua Univ., Hsinchu, Taiwan

**C. K. Cheng, K. Y. Lin, and M. Hong\***

Grad. Inst. of Appl. Phys., National Taiwan Univ., Taipei, Taiwan

**S. W. Lien, and T. R. Chang**

Dept. of Phys., National Cheng Kung Univ., Taipei, Taiwan

**C. M. Cheng, and C. H. Hsu**

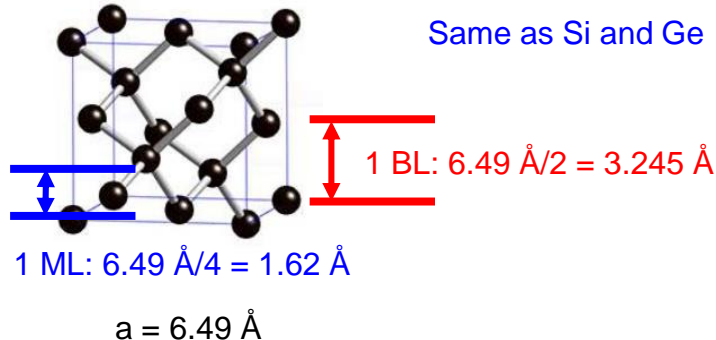
National Synchrotron Radiation Research Center, Hsinchu, Taiwan



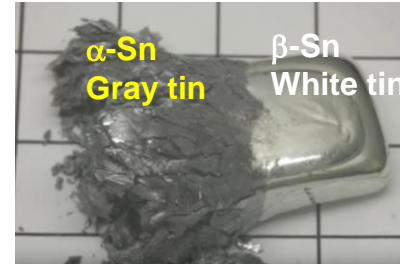
# Introduction: crystal structure of Sn

## $\alpha$ -Sn Gray tin

face centered cubic (diamond)



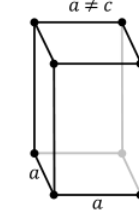
Low temperature phase



## $\beta$ -Sn White tin

tetragonal

High temperature phase



$$a = 5.83 \text{ \AA}$$

$$c = 3.18 \text{ \AA}$$

below  $\leftarrow$  Phase transition temperature  $\rightarrow$  above

bulk crystal:  $13.2^\circ\text{C}$

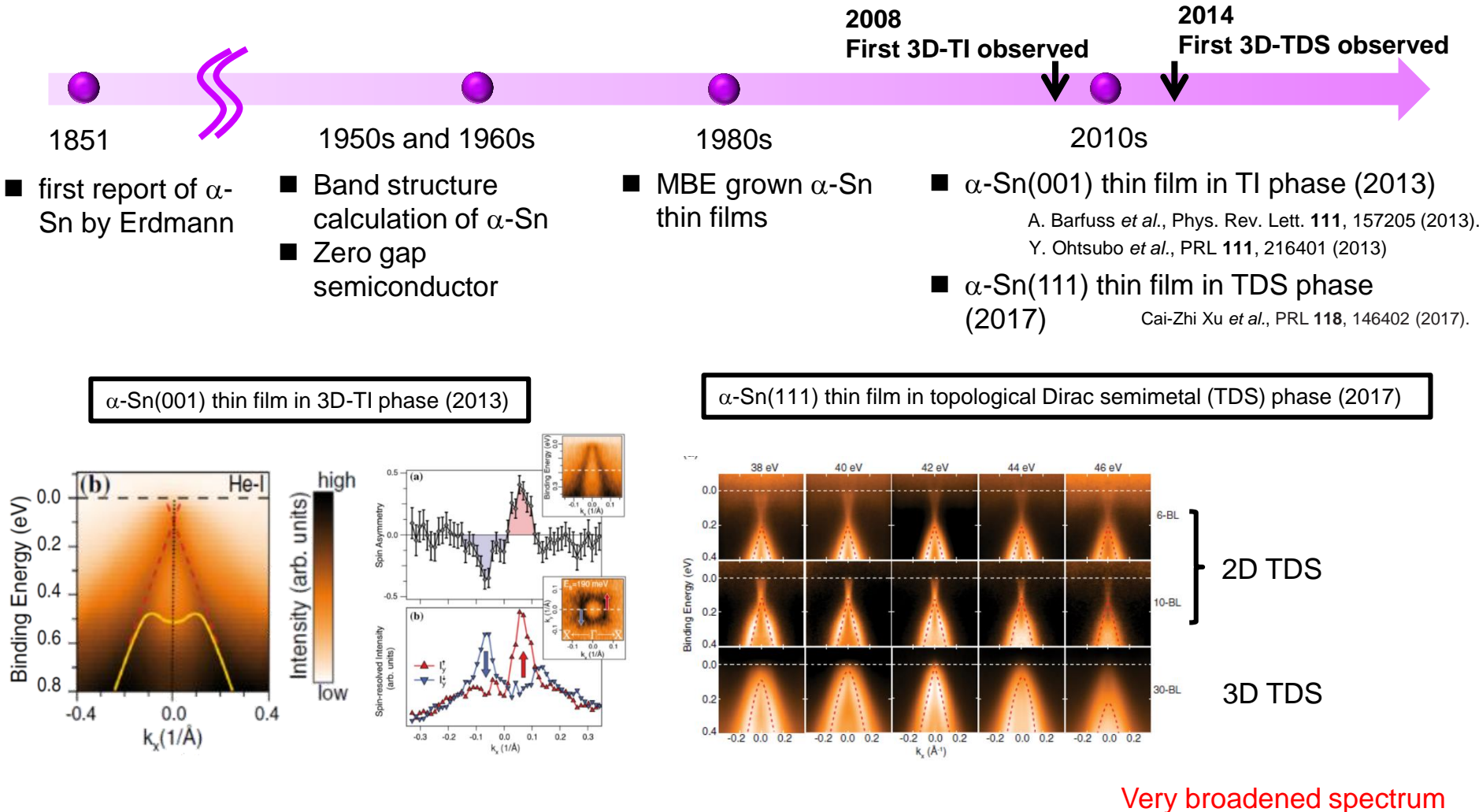
thin film:  $70 - 170^\circ\text{C}$

- on nearly lattice matched substrates (InSb, CdTe)
- depend on film thickness and orientation

R. F. C. Farrow, Mat. Res. Soc. Symp. Proc. **37**, 275. (1984).

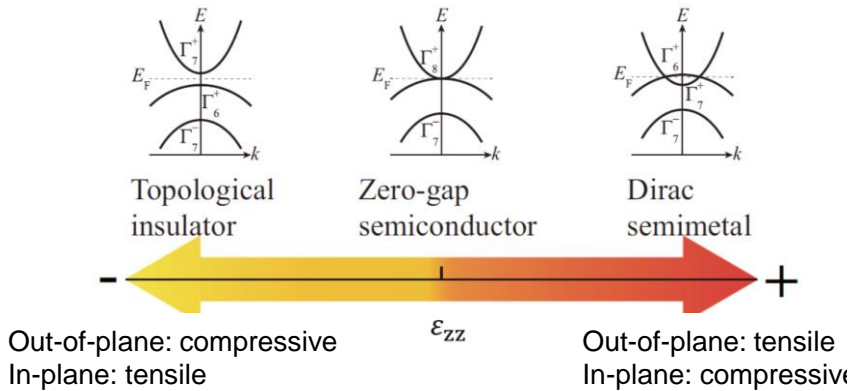
T. Osaka *et al.*, Phys. Rev. B **50**, 7567 (1994).

# Introduction: discovery of $\alpha$ -Sn

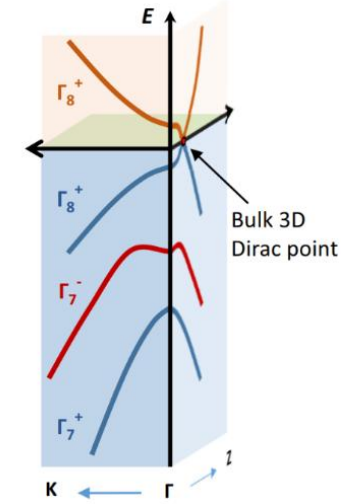
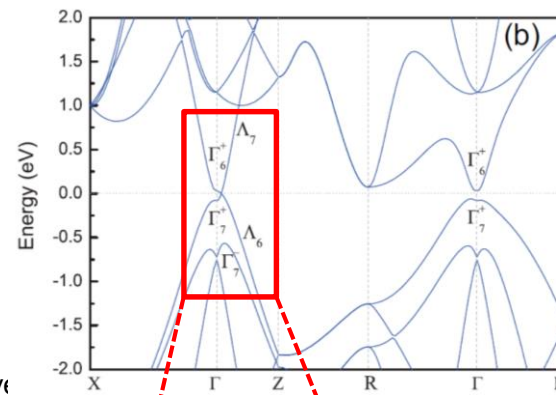


# Introduction: discovery of $\alpha$ -Sn

Predictions of  $\alpha$ -Sn(001) as a TDS under in-plane compressive strain

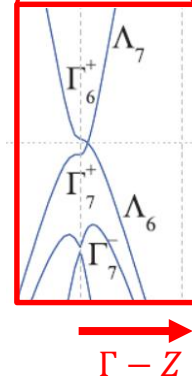


Huaqing Huang and Feng Liu, *Phys. Rev. B* **95**, 201101(R) (2017).



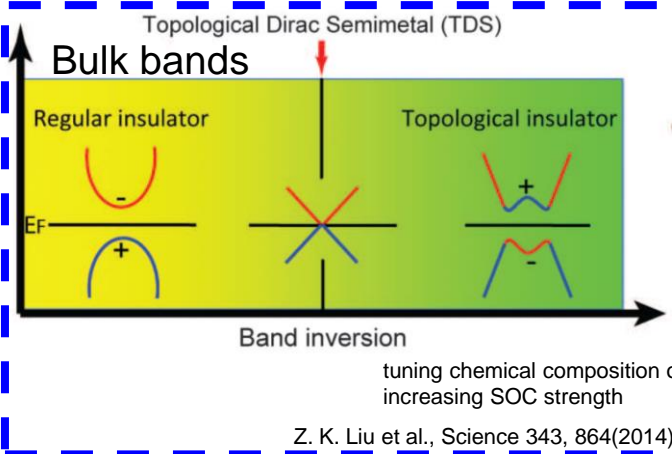
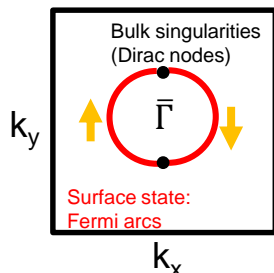
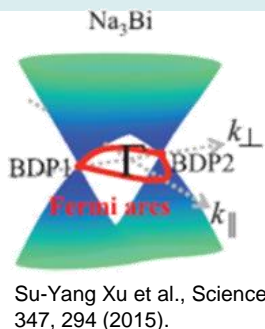
M. R. Scholz et al., *Phys. Rev. B* **97**, 075101 (2018).

- Band crossing along  $\Gamma - Z$
- Still lack of experimental prove

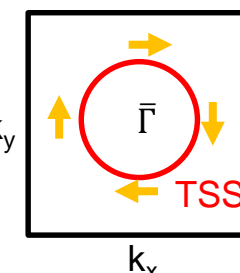
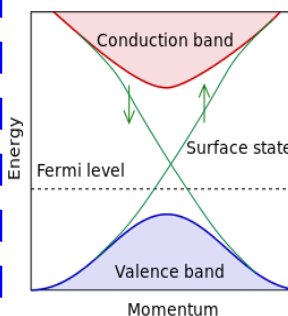


# Introduction: topological insulator and topological Dirac semimetal

## Topological Dirac semimetal (TDS)



## Topological insulator (TI)



2D TDS: graphene

3D TDS (3D analog of graphene):

Na<sub>3</sub>Bi (C3 symmetry), Cd<sub>3</sub>As<sub>2</sub> (C4 symmetry)

□ Gap closed at Dirac node

□ Spin-polarized Fermi arcs connecting Dirac nodes

2D TI:

HgTe/CdTe quantum well

3D TI:

Bi<sub>x</sub>Sb<sub>1-x</sub>, Bi<sub>2</sub>Se<sub>3</sub>, Bi<sub>2</sub>Te<sub>3</sub>, ...

□ Fully gapped bulk state

□ A chiral edge/surface state connecting bulk conduction and valence band

# Motivation

- Expected to be an ideal **elemental** topological material (TM) with **less material defects** compared with binary or ternary compound TM
- Non-toxic group IV material
  - 1. easy to tackle
  - 2. greater potential in combining with current semiconductor technology
- Large spin-to-charge conversion efficiency ( $\lambda_{IEE} \sim 2.1$  nm) at room temperature compared to other conventional TI hetero-structure ( $\lambda_{IEE} \sim 0.009\text{-}0.43$  nm)
  - J.-C. Rojas-Sánchez *et al.*, PRL **116**, 096602 (2016).
  - novel spintronic devices
- Phase transition from topological insulator to topological Dirac semimetal by strain manipulation
  - a fascinating material for studying topological phase transition

Cai-Zhi Xu *et al.*, PRL **118**, 146402 (2017).  
Huaqing Huang and Feng Liu, PRB **95**, 201101(R) (2017).  
Dongqin Zhang *et al.*, PRB **97**, 195139 (2018).

# Band structure of $\alpha$ -Sn(001) studied by ARPES

## $\alpha$ -Sn on InSb(001)

Prof. J. Schafer and R. Claessen's group in Germany

A. Barfuss et al., PRL 111, 157205 (2013)

Victor A. Rogalev et al., PRB 95, 161117(R) (2017)

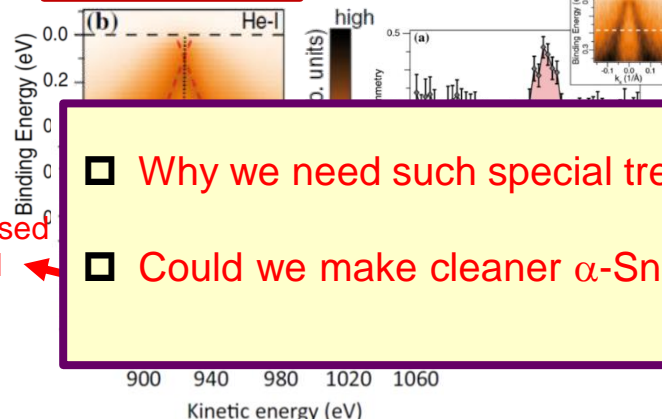
M. R. Scholz et al., PRB 97, 075101 (2018)

Spin-momentum  
locked surface state

2D state of TSS

Dirac-like TSS

Te doped  $\alpha$ -Sn  
InSb(001)-c(8x2)



Te peaks increased  
at 60° off normal

- Why we need such special treatments to observe the TSS of  $\alpha$ -Sn(001)?
- Could we make cleaner  $\alpha$ -Sn(001) films for the study of topological state?

Dr. Amina Taleb-Ibrahimi and Prof. A. Fert's group in France

Y. Ohtsubo et al., PRL 111, 216401 (2013)

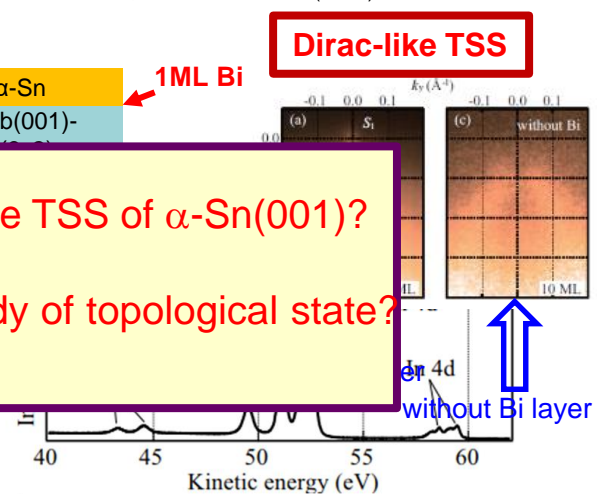
J.-C. Rojas-Sánchez et al., PRL 116, 096602 (2016)

Q. Barbedienne et al., arXiv:1807.11377 (2018)

Dirac-like TSS

$\alpha$ -Sn  
InSb(001)-

1ML Bi



- InSb wafer cleaned by sputtering and annealing
- No TSS observed without resorting to Te atoms or Bi buffer layer
- No clear evidence of TDS phase found in  $\alpha$ -Sn(001) as predicted in calculation
- Severe In diffusion problem  $\rightarrow$  p-type pristine surface
- Te or Bi atoms segregated to the top of Sn films

# Sample preparation

- InSb(001) substrate cleaning using CP4 solution

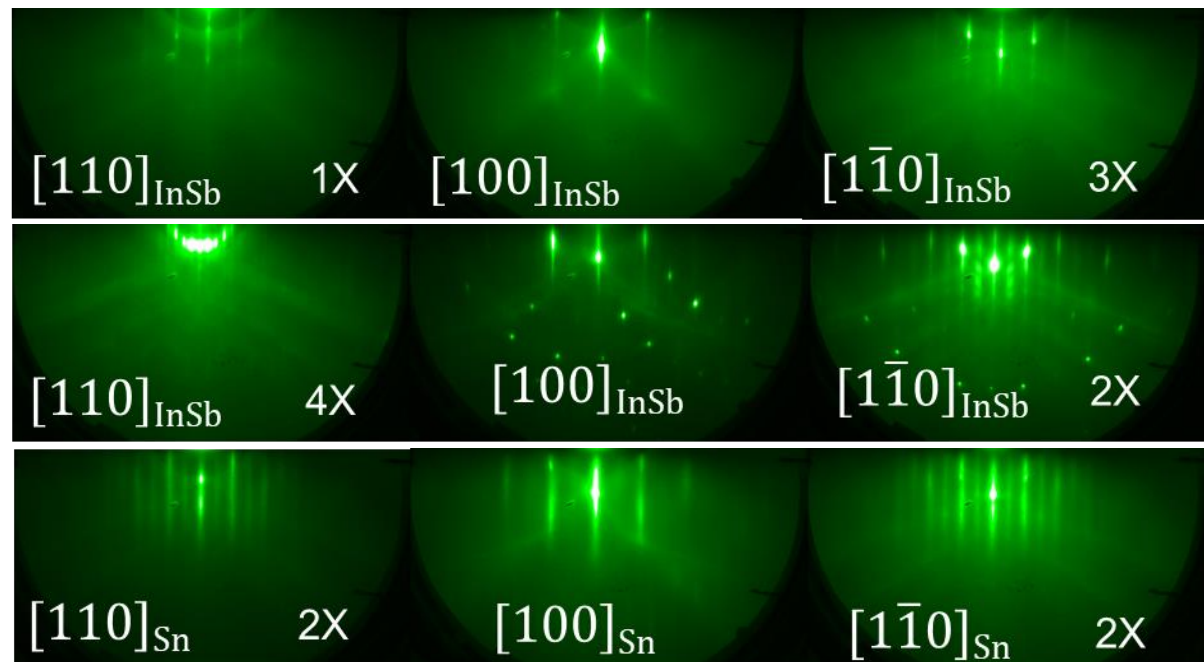
- Native oxides desorption under Sb flux at  $T_s \sim 450$  °C

- Growth of InSb epilayer

at  $T_s$  of 380 to 400 °C

- Growth of  $\alpha$ -Sn film

at  $T_s$  of ~ 0 to 100 °C

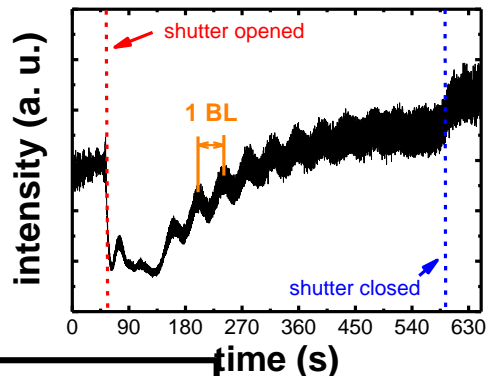


- ***In-situ* measurements:** LEED, ARPES, XPS, STM

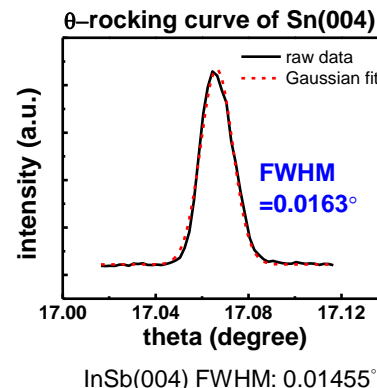
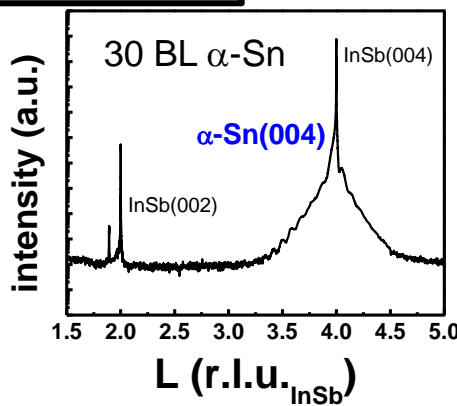
- ***Ex-situ* measurements:** XRD, AFM

# Crystal structure study

RHEED oscillation during Sn growth

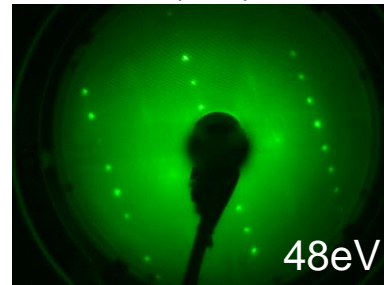


X-ray diffraction

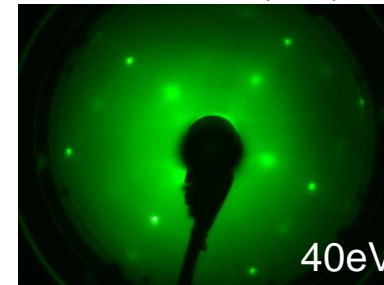


LEED patterns

InSb(001)-4x2



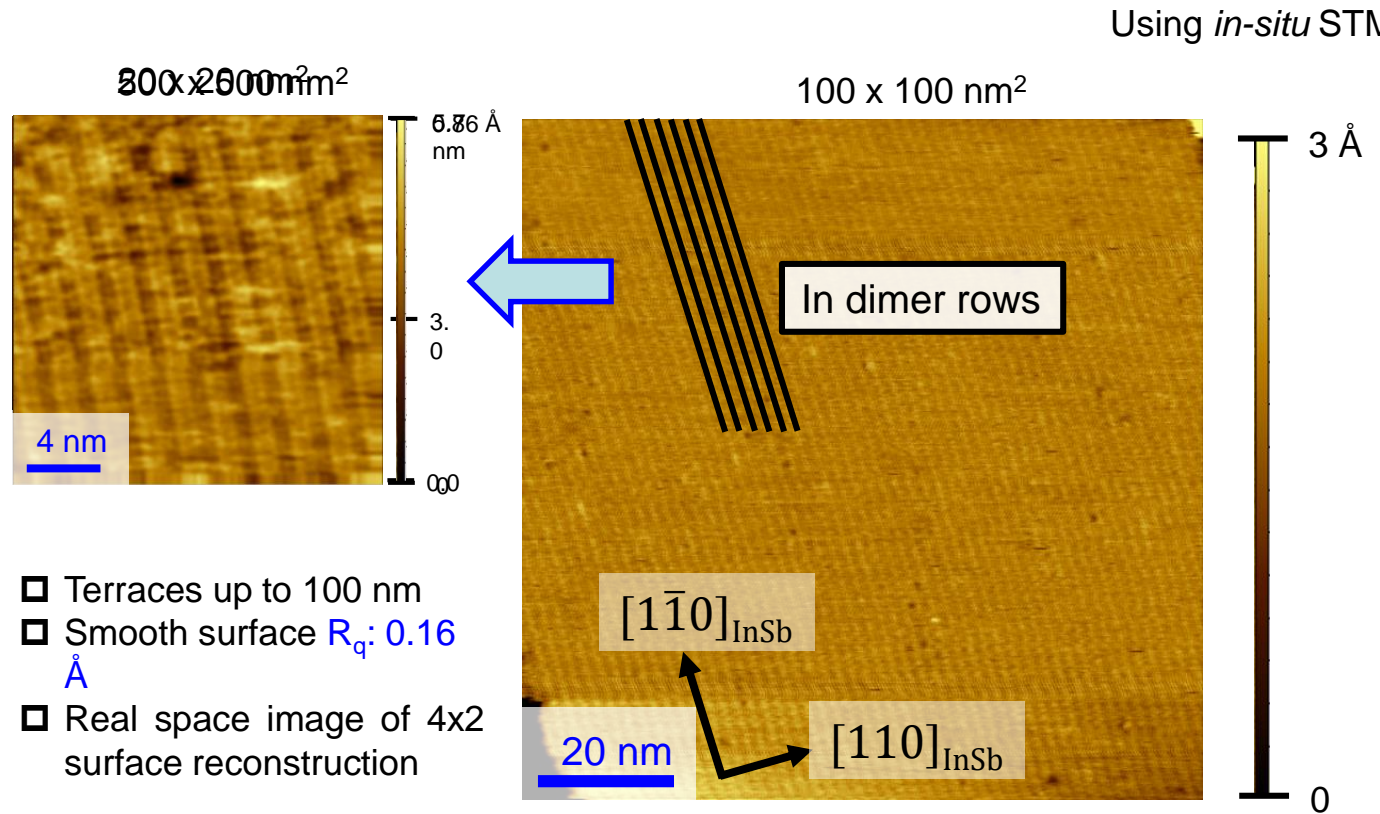
Two-domain Sn(001)-2x1



Four fold symmetry

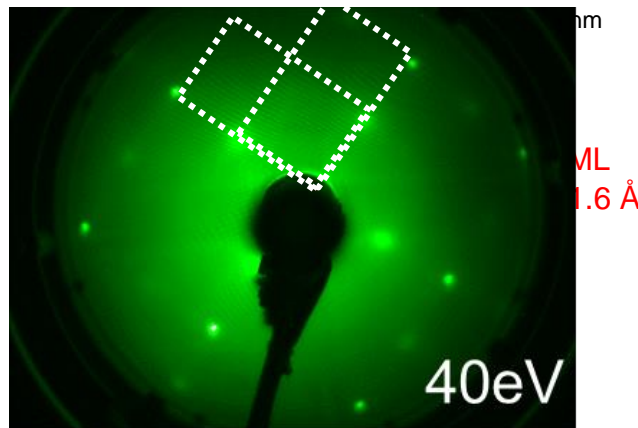
- Layer-by-layer growth of Sn with RHEED oscillation observed in every sample
- Smooth surface
- Sharp RHEED and LEED patterns with two-domain 2x1 surface reconstruction
- Pure α phase Sn with excellent crystallinity

# Surface morphology: InSb(001)-4x2



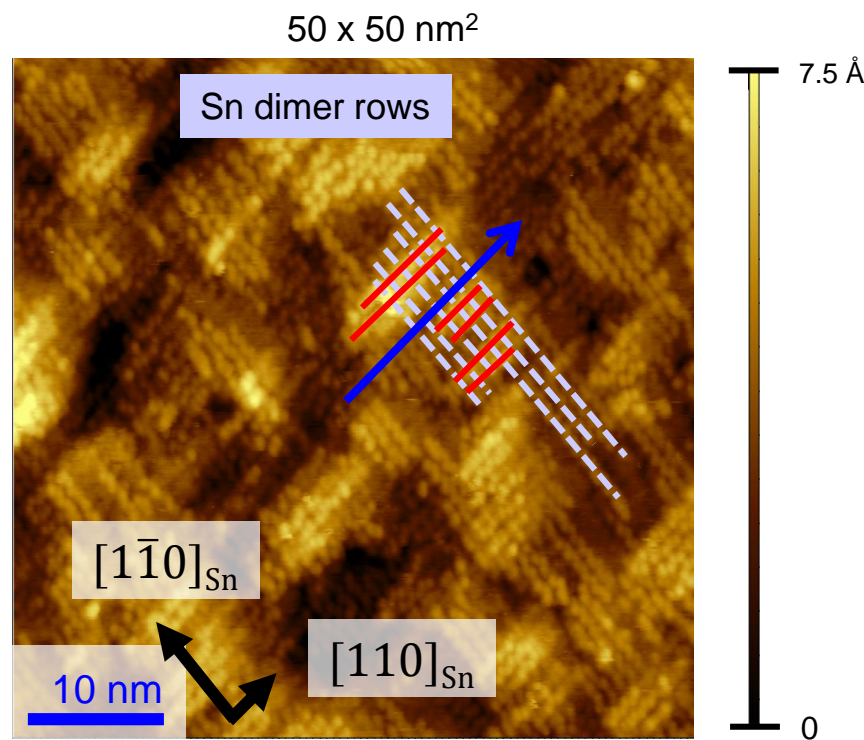
# Surface morphology: $\alpha$ -Sn(001)-2x1

Two-domain Sn(001)-2x1  
spacing of Sn dimer rows

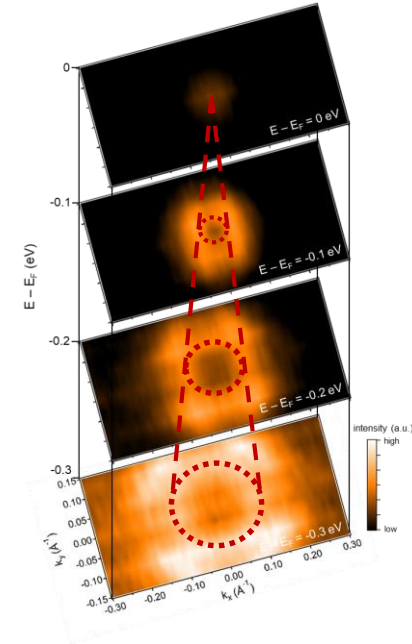
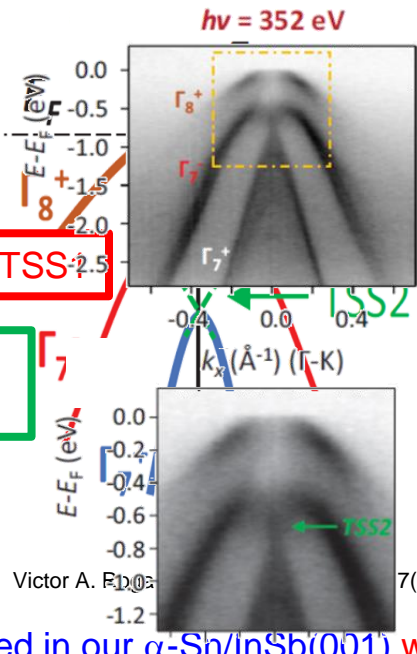
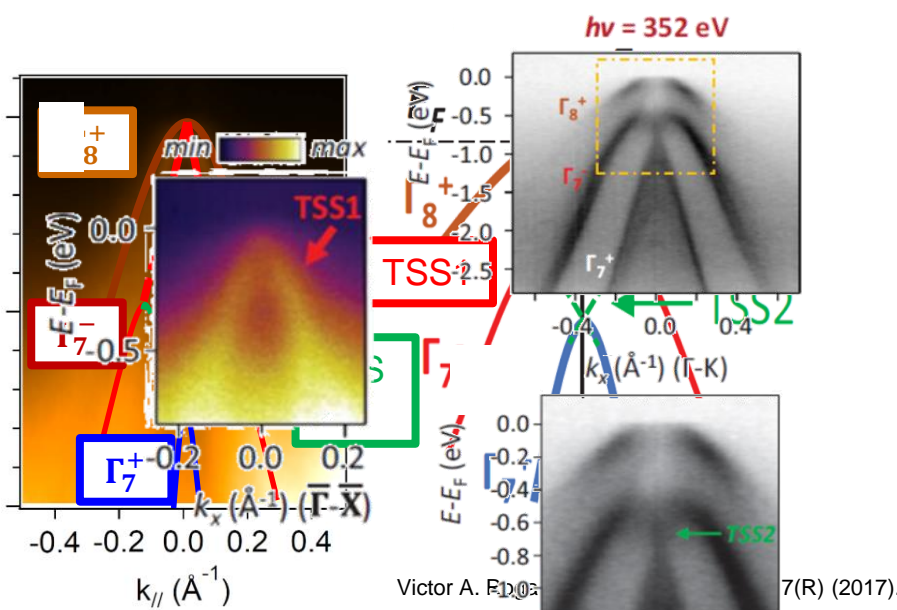
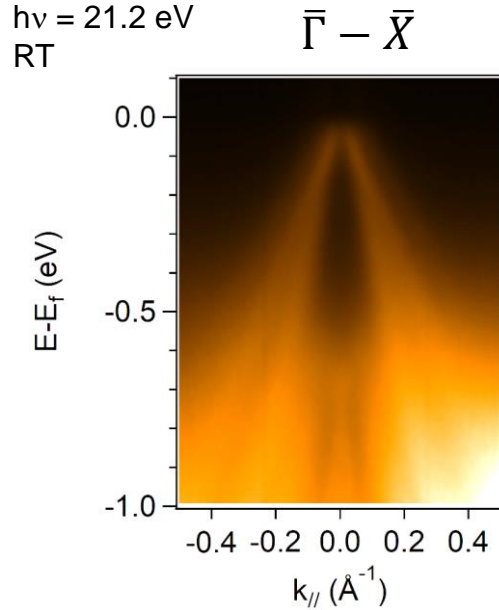


- Smooth surface  $R_q$ : 1.3 Å
- Real space image of 2x1 surface reconstruction
- Consistent with the observation in LEED

Using *in-situ* STM



# ARPES spectra of 30 BL $\alpha$ -Sn/InSb(001)



- Dirac-like state and three bulk bands were observed in our  $\alpha$ -Sn/InSb(001) without adding Te in Sn or using Bi buffer layer.
- The Fermi velocity ( $v_F$ ) of TSS1 is  $(6.5 - 7) \times 10^5 \text{ m/s}$ , which is similar to reported value  $(7.3 \times 10^5 \text{ m/s})$ , larger than the one of  $\text{Bi}_2\text{Se}_3$   $(2.9 \times 10^5 \text{ m/s})$  and smaller than the one of graphene  $(1 \times 10^6 \text{ m/s})$ .

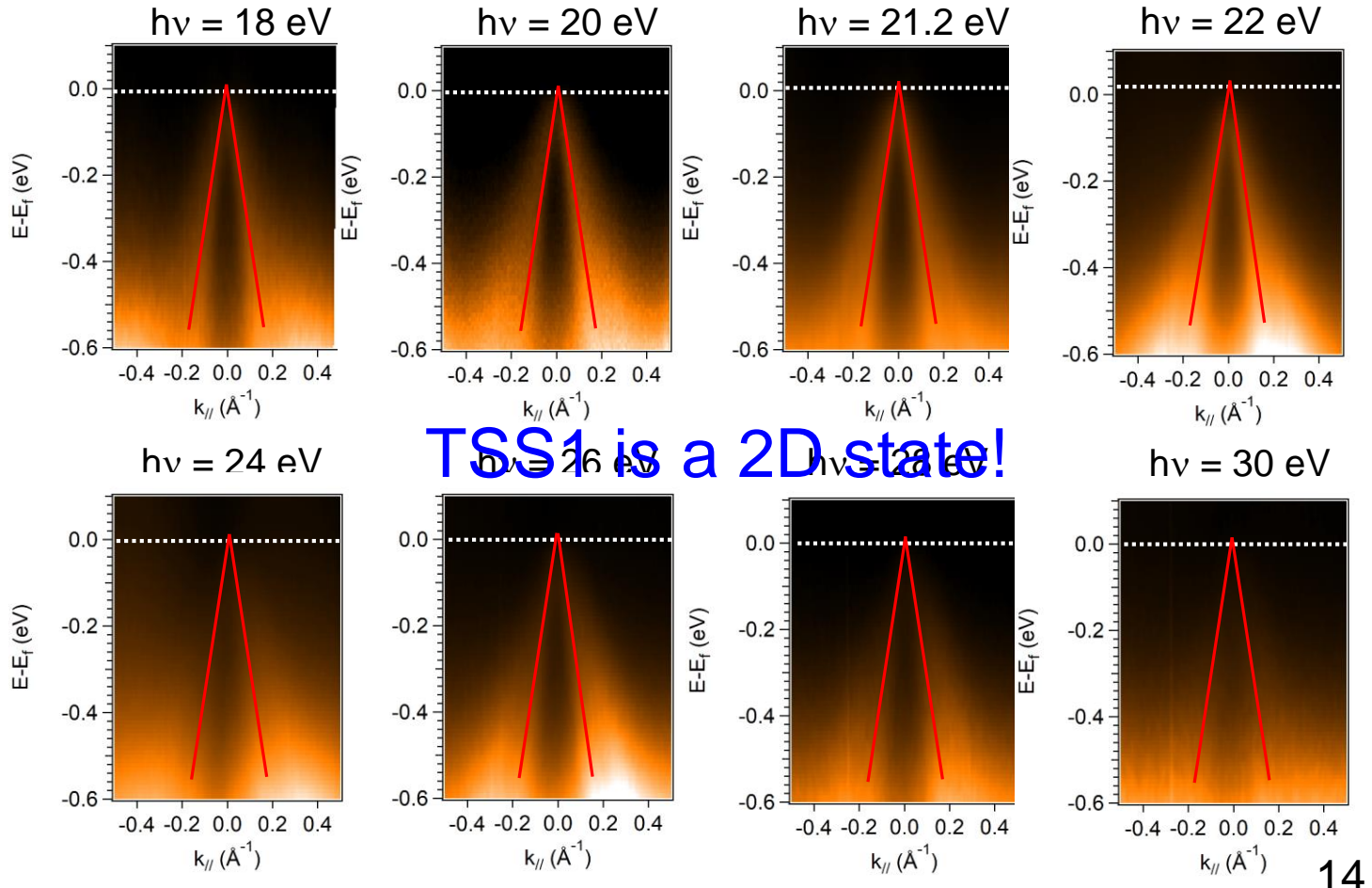
Victor A. Rogalev et al., Phys. Rev. B **95**, 161117(R) (2017).

Y. Ohtsubo et al., Phys. Rev. Lett. **111**, 216401 (2013).

K. Kuroda et al., Phys. Rev. Lett. **105**, 146801 (2010).

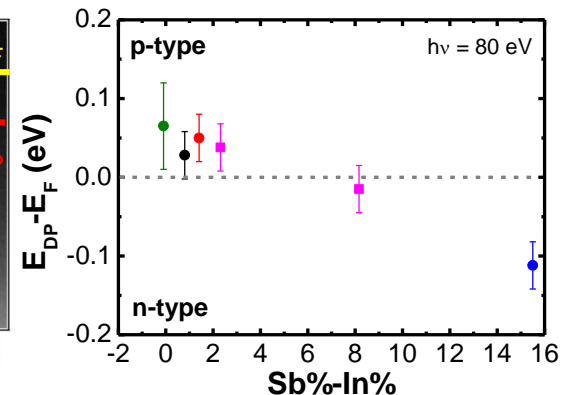
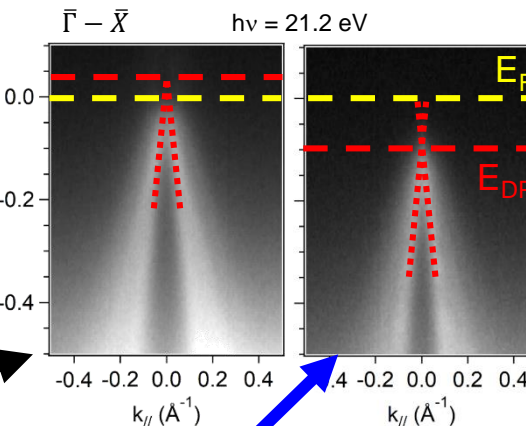
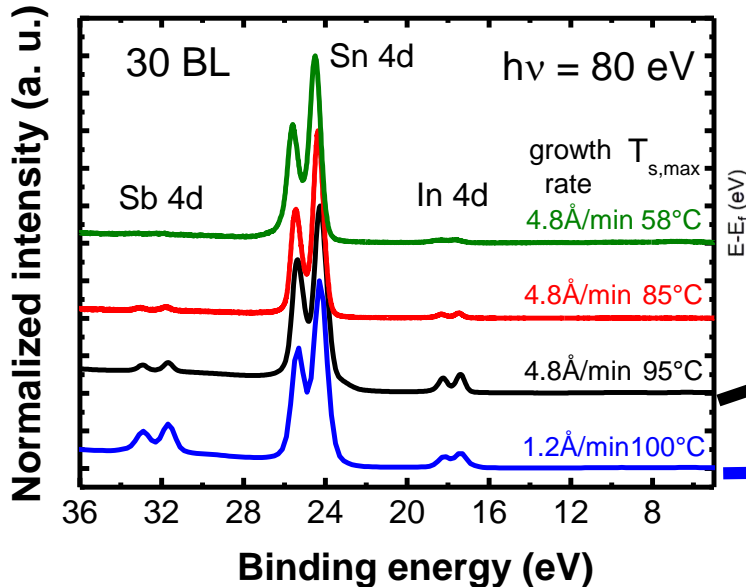
C. Berger et al., Science **312**, 1191 (2006).

# Energy dependent ARPES spectra of $\alpha$ -Sn



14

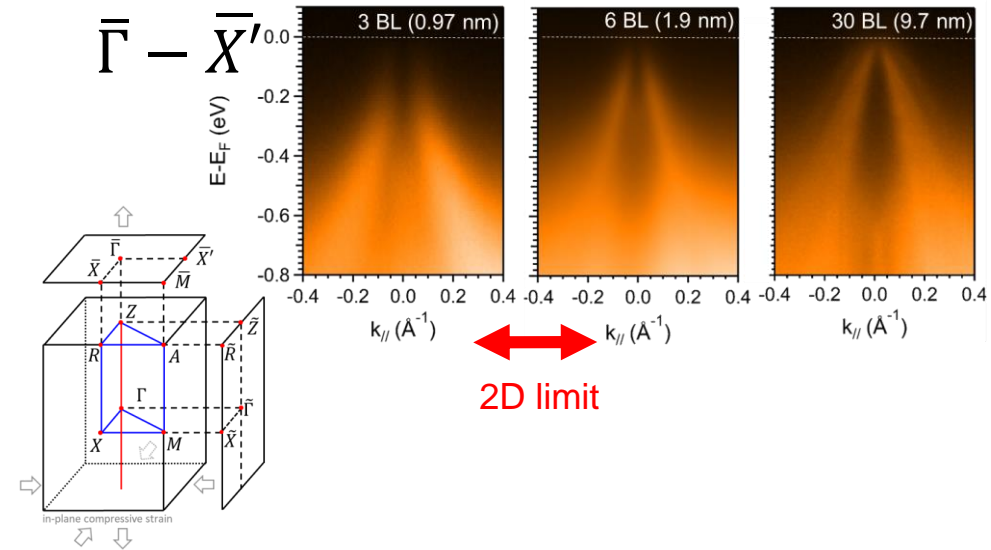
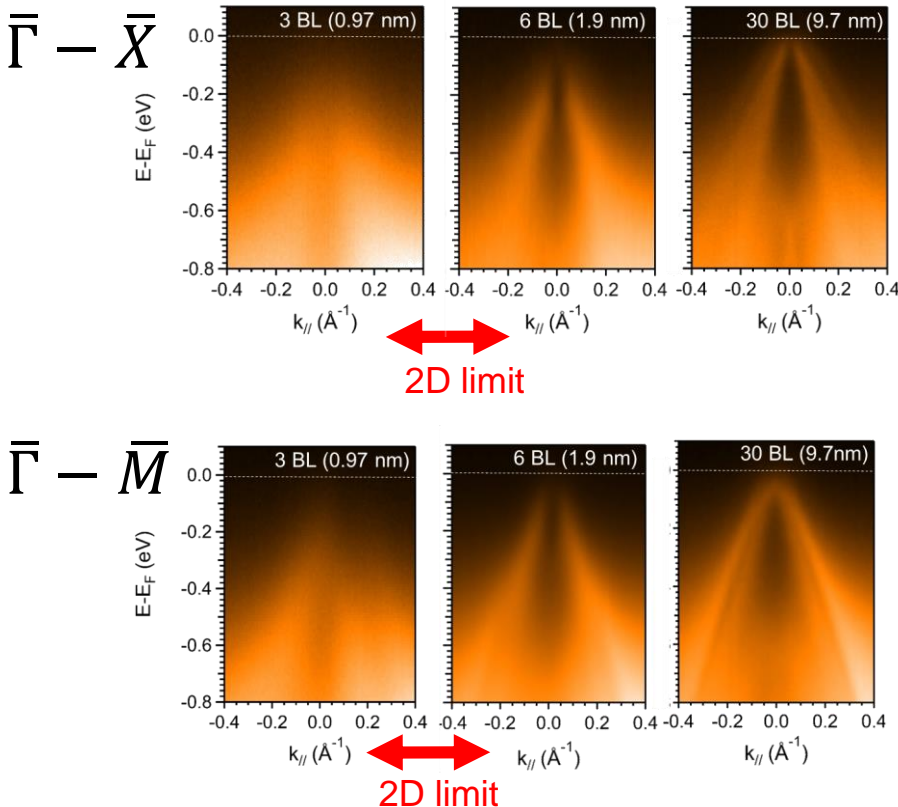
# X-ray photoemission study



- Diffusion problem minimized by lowering substrate temperature
- Fermi level of  $\alpha$ -Sn varied from p-type to n-type by controlling the inter-diffusion without severe degradation of TSS

# Thickness dependent ARPES spectra of $\alpha$ -Sn(001): 3-30 BL

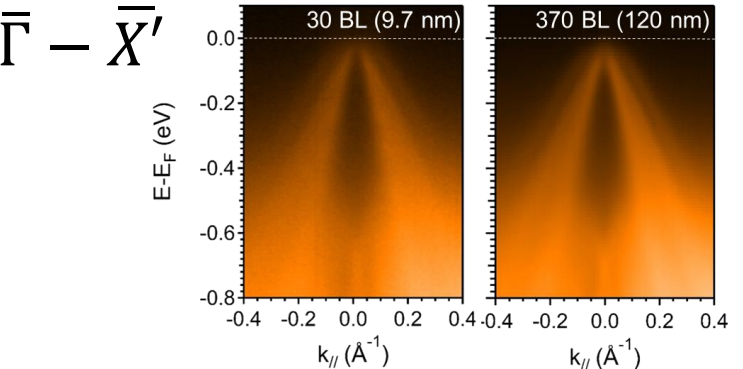
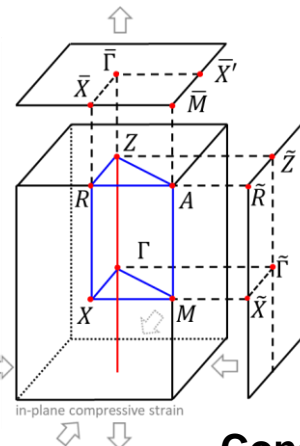
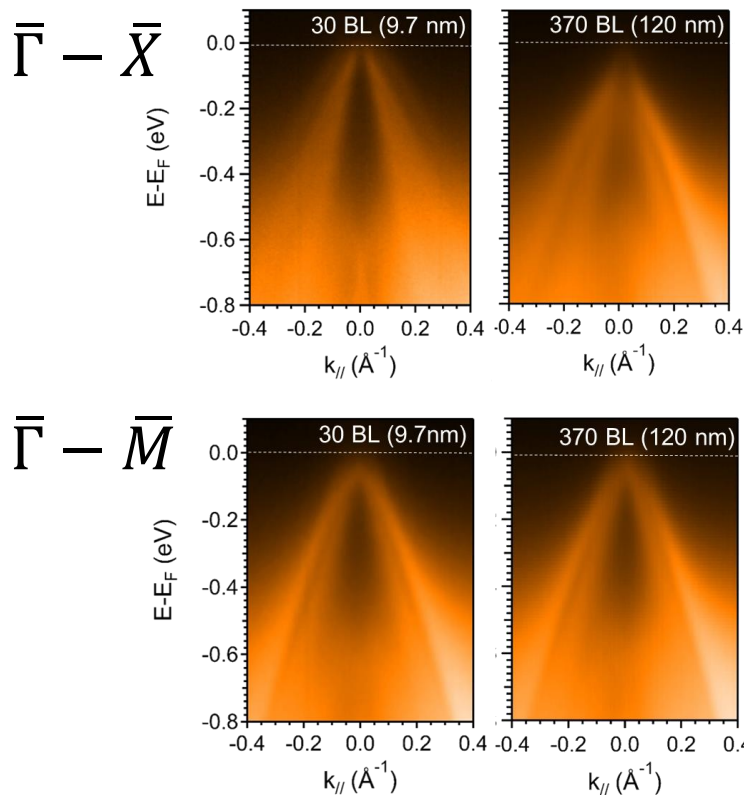
$h\nu = 21.2$  eV RT



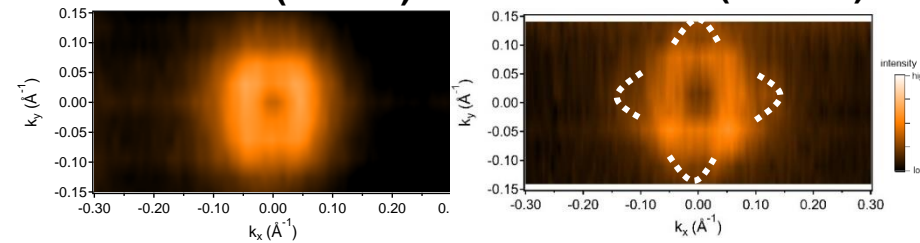
- TSS state becomes very weak and broadened in 6 BL sample
- No TSS observed in 3 BL sample
- 2D limit between 4-6 BL

# Thickness dependent ARPES spectra of $\alpha$ -Sn(001): 30 BL and 370 BL

$h\nu = 21.2$  eV RT

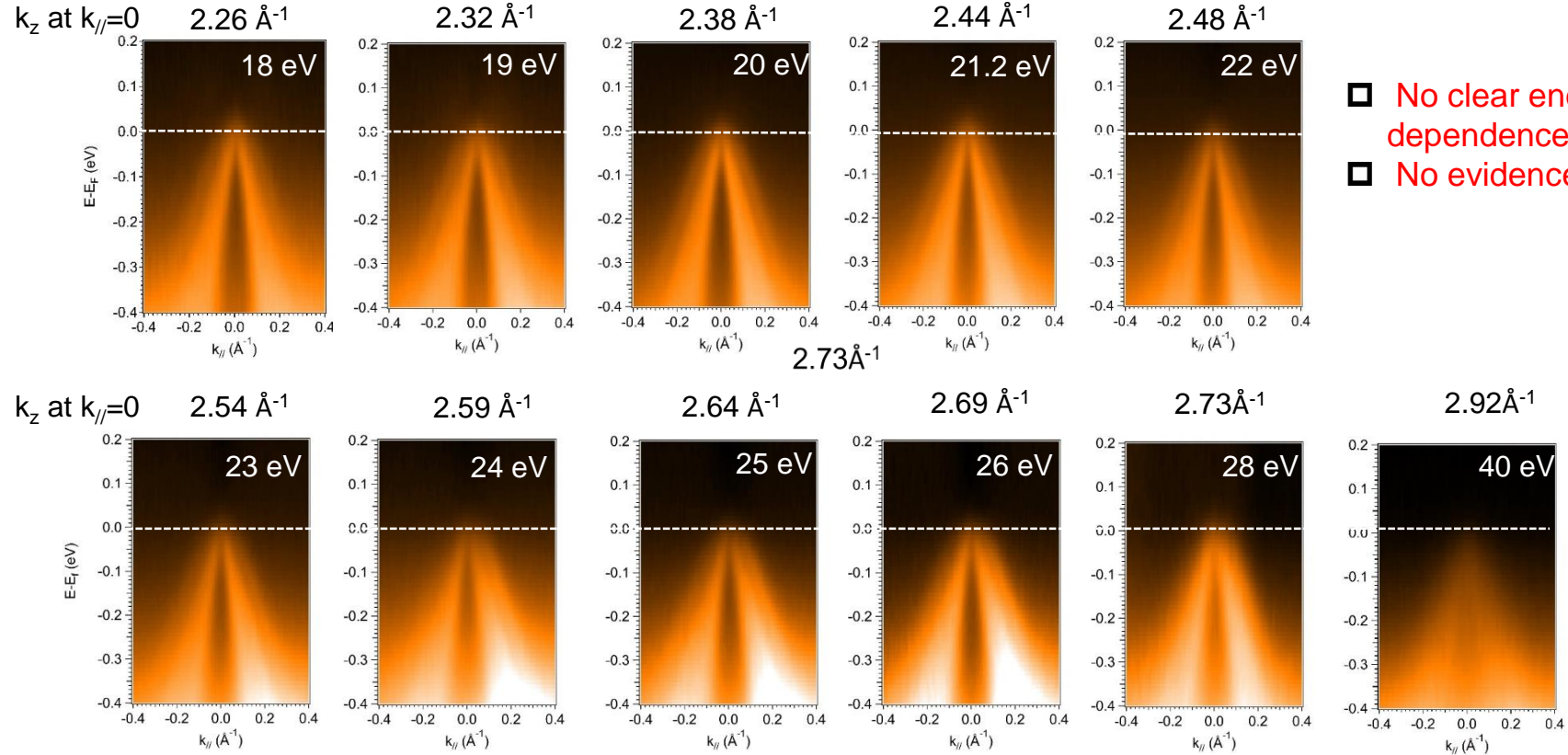


Constant energy contour ( $E - E_F = -100$  meV)  
30 BL (9.7 nm)      370 BL (120 nm)



□ More distinct bands

# Energy-dependent analysis of 370 BL (120 nm) $\alpha$ -Sn/InSb(001)

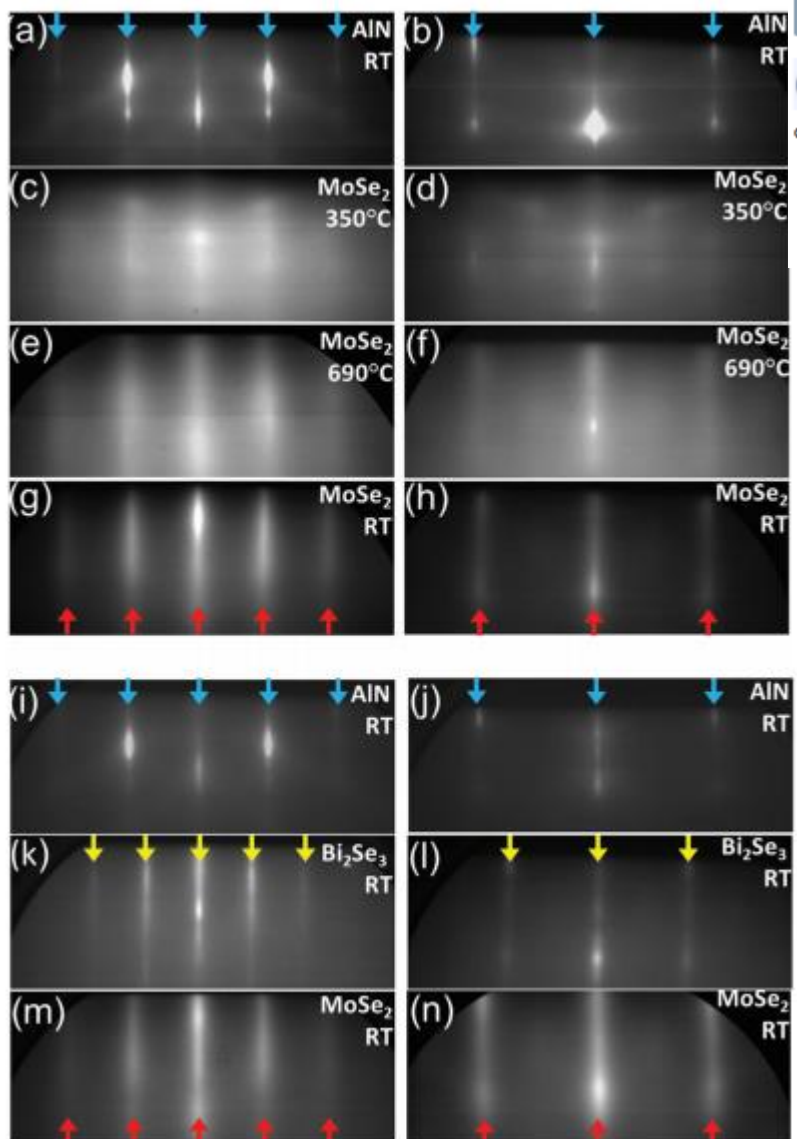


# **Thank you for your attention!**

[11̄20]

[1̄100]

Nanoscale



PAPER



Cite this: Nanoscale, 2015, 7, 7896

[View Article Online](#)  
[View Journal](#) | [View Issue](#)

## High-quality, large-area MoSe<sub>2</sub> and MoSe<sub>2</sub>/Bi<sub>2</sub>Se<sub>3</sub> heterostructures on AlN(0001)/Si(111) substrates by molecular beam epitaxy†

E. Xenogiannopoulou,<sup>a</sup> P. Tsipas,<sup>a</sup> K. E. Aretouli,<sup>a</sup> D. Tsoutsou,<sup>a</sup> S. A. Giannini,<sup>a</sup> C. Bazioti,<sup>b</sup> G. P. Dimitrakopoulos,<sup>b</sup> Ph. Komninou,<sup>b</sup> S. Brems,<sup>c</sup> C. Huyghebaert,<sup>c</sup> I. P. Radu<sup>c</sup> and A. Dimoulas<sup>a\*</sup>

**Fig. 1** RHEED patterns of: (a–h) 1 ML MoSe<sub>2</sub> deposited on AlN(0001) by the 2 step-process, and (i–n) 2 ML MoSe<sub>2</sub> deposited on a 5 QL Bi<sub>2</sub>Se<sub>3</sub> buffer layer, epitaxially grown on AlN(0001). (a) and (i) show the bare AlN (0001) pattern along the [11̄20] azimuth and (b and j) bare AlN(0001) along the [1̄100] azimuth. (c) and (d) are recordings at 350 °C after the deposition of MoSe<sub>2</sub>, (e) and (f) are recordings at 690 °C after the post-deposition annealing step, while (g) and (h) present the MoSe<sub>2</sub> film on AlN after final cooling down to RT. In (e) and (f) MoSe<sub>2</sub> becomes highly crystalline with the respective crystal orientations aligned to those of AlN, which is clearly observed after cooling down in (g) and (h). (k) and (l) show a 5 QL Bi<sub>2</sub>Se<sub>3</sub> buffer layer grown epitaxially on AlN(0001) at 300 °C with high crystalline quality, (m) and (n) show that MoSe<sub>2</sub> deposited on the Bi<sub>2</sub>Se<sub>3</sub> buffer layer at 300 °C grows epitaxially, with [11̄20]<sub>MoSe<sub>2</sub></sub>//[11̄20]<sub>Bi<sub>2</sub>Se<sub>3</sub></sub> and [1̄100]<sub>MoSe<sub>2</sub></sub>//[1̄100]<sub>Bi<sub>2</sub>Se<sub>3</sub></sub>. The blue and yellow downward arrows show AlN and Bi<sub>2</sub>Se<sub>3</sub> streaks, respectively. The red upward arrows show MoSe<sub>2</sub> streaks.

# Topological insulator $\text{Bi}_2\text{Se}_3$ thin films grown on double-layer graphene by molecular beam epitaxy

Can-Li Song,<sup>1,2</sup> Yi-Lin Wang,<sup>1</sup> Ye-Ping Jiang,<sup>1,2</sup> Yi Zhang,<sup>1</sup> Cui-Zu Chang,<sup>1,2</sup> Lili Wang,<sup>1</sup> Ke He,<sup>1</sup> Xi Chen,<sup>2</sup> Jin-Feng Jia,<sup>2</sup> Yanyu Wang,<sup>2</sup> Zhong Fang,<sup>1</sup> Xi Dai,<sup>1</sup> Xin-Cheng Xie,<sup>1</sup> Xiao-Liang Qi,<sup>3</sup> Shou-Cheng Zhang,<sup>3</sup> Qi-Kun Xue,<sup>1,2,a)</sup> and Xucun Ma<sup>1</sup>

<sup>1</sup>Institute of Physics, Chinese Academy of Sciences, Beijing 100190, People's Republic of China

<sup>2</sup>Department of Physics, Tsinghua University, Beijing 100084, People's Republic of China

<sup>3</sup>Department of Physics, Stanford University, Stanford, California 94305-4045, USA

(Received 6 July 2010; accepted 9 September 2010; published online 7 October 2010)

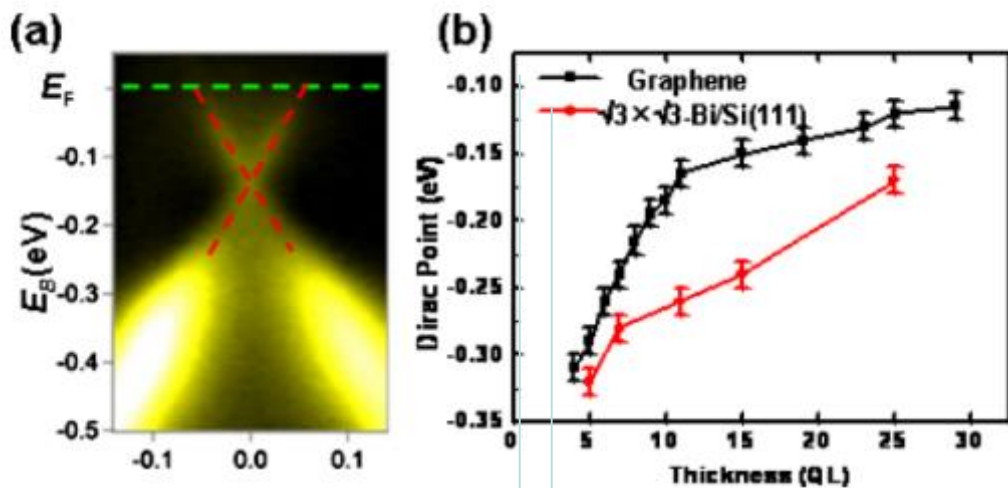
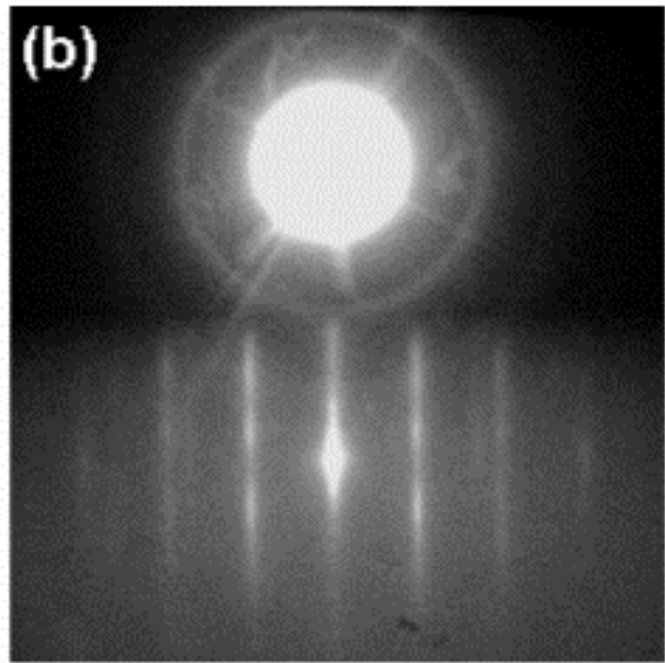


FIG. 2. (Color online) (a) ARPES intensity map of the 26 QL film along the  $\Gamma$ -K direction. The dotted line indicates the Fermi level, and the topological surface states, respectively. (b) Thickness-dependent surface Dirac point of  $\text{Bi}_2\text{Se}_3$  films on graphene and Si substrates.